Reaction of Neuronal Nitric-Oxide Synthase with 2,6-Dichloroindolphenol and Cytochrome c^{3+}: Influence of the Electron Acceptor and Binding of Ca^{2+}-Activated Calmodulin on the Kinetic Mechanism†

Kirsten R. Wolthers‡ and Michael I. Schimerlik*,‡,§

Department of Biochemistry and Biophysics and Environmental Health Sciences Center, Oregon State University, Corvallis, Oregon 97331

Received October 9, 2000; Revised Manuscript Received January 5, 2001

ABSTRACT: Binding of Ca^{2+}-activated calmodulin (Ca^{2+}-CaM) to neuronal nitric-oxide synthase (nNOS) increases the rate of 2,6-dichloroindolphenol (DCIP) reduction 2−3-fold and that of cytochrome c^{3+} 10−20-fold. Parallel initial velocity patterns indicated that both substrates were reduced via two-half reactions in a ping-pong mechanism. Product and dead-end inhibition data with DCIP were consistent with an iso ping-pong bi-bi mechanism; however, product and dead-end inhibition studies with cytochrome c^{3+} were consistent with the (two-site) ping-pong mechanism previously described for the NADPH−cytochrome P450 reductase-catalyzed reduction of cytochrome c^{3+} [Sem, D., and Kasper, C. (1994) *Biochemistry 33*, 12012−12021]. Dead-end inhibition by 2′-adenosine monophosphate (2′AMP) was competitive versus NADPH for both electron acceptors, although the value of the slope inhibition constant, K_{is}, was 25−30-fold greater with DCIP as the substrate than with cytochrome c^{3+}. The difference in the apparent affinity of 2′AMP is proposed to result from a rapidly equilibrating isomerization step that occurs in both mechanisms prior to the binding of NADPH. Thus, initial velocity, product, and dead-end inhibition data were consistent with a di-iso ping-pong bi-bi and an iso (two-site) ping-pong mechanism for the reduction of DCIP and cytochrome c^{3+}, respectively. The presence Ca^{2+}-CaM did not alter the proposed kinetic mechanisms. The activated cofactor had a negligible effect on $(k_{cat}/K_m)_{NADPH}$, while it increased $(k_{cat}/K_m)_{DCIP}$ and $(k_{cat}/K_m)_{cytc}$ 4.5- and 23-fold, respectively.

Nitric oxide (NO)[1] is a ubiquitous molecule involved in a diverse array of physiological and pathological roles (*1*−*5*). NO is synthesized in mammals by the NO-synthases, a family of three homodimeric enzymes. Each of the isoforms consumes 1.5 equiv of NADPH and 2 equiv of O_2 in the five-electron oxidation of L-arginine to produce NO and L-citrulline (*6*, *7*). The enzymes can be classified into two distinct groups according to regulation of transcriptional expression and dependence on intracellular Ca^{2+} concentrations. The constitutively expressed neuronal (nNOS) and endothelial (eNOS) isoforms require an increase in Ca^{2+} levels to promote the subsequent binding of Ca^{2+}-activated calmodulin (Ca^{2+}-CaM) for NO synthesis (*8*). The inducible isoform (iNOS) is transcriptionally regulated by the action of cytokines, and its NO synthesis activity is independent of Ca^{2+} concentration since CaM is tightly bound to this isoform even at basal cellular levels of the divalent cation (*9*).

The CaM-binding domain, located at the center of the NOS polypeptide subunit, tethers the oxygenase domain to the reductase domain (*9*−*11*). The reductase domain is structurally similar to NADPH−cytochrome P450 oxidoreductase (CPR) since each polypeptide contains 1 equiv each of FAD and FMN and the binding site for NADPH (*12*, *13*). The oxygenase domain is structurally unique and contains a P450-type heme, the binding site for the cofactor (6*R*)-5,6,7,8-tetrahydro-L-biopterin (H_4B), and the substrate L-arginine (*14*−*17*). For the constitutive isoforms, the binding of Ca^{2+}-CaM is essential for NO synthesis, because it triggers the electron transfer between the flavins in the reductase domain and the heme in the oxygenase domain (*18*, *19*). Evidence from several laboratories indicates that the NOS reductase domain and CPR share the same mechanism of electron transfer to the heme. The FAD and FMN redox centers of both enzymes shuttle two electrons from the oxidation of NADPH to a one-electron heme acceptor (*13*). In the absence of NADPH, both CPR and NOS maintain an air-stable one-electron-reduced state (FAD-FMNH•) (*20*, *21*), which is unable to reduce the heme (*22*, *23*). The donation of two electrons through the oxidation of NADPH reduces either enzyme to the three-electron-reduced state. The flavins then subsequently reduce the P-450 heme in two one-electron

† This work was supported by Grant ES00210 from the National Institute of Environmental Health Sciences.

* To whom correspondence should be addressed: Department of Biochemistry and Biophysics, Agricultural and Life Sciences Building 2011, Oregon State University, Corvallis, OR 97331. Telephone: (541) 737-2029. Fax: (541) 737-0481. E-mail: schimerm@ucs.orst.edu.

‡ Department of Biochemistry and Biophysics.

§ Environmental Health Sciences Center.

[1] Abbreviations: NO, nitric oxide; nNOS, neuronal nitric-oxide synthase; eNOS, endothelial NOS; iNOS, inducible NOS; Ca^{2+}-CaM, Ca^{2+}-activated calmodulin; CPR, NADPH−cytochrome P450 oxidoreductase; H_4B, (6*R*)-5,6,7,8-tetrahydrobiopterin; FeCN, ferricyanide; DCIP, 2,6-dichloroindolphenol; cytc, cytochrome c^{3+}; 2′AMP, 2′-adenosine monophosphate; $DCIP_{ox}$, oxidized form of DCIP; $DCIP_{red}$, reduced form of DCIP.

10.1021/bi0023495 CCC: $20.00
Published on Web 03/22/2001

transfers, returning the enzyme to the one-electron-reduced state (*24*, *25*). Therefore, during turnover it is proposed that NOS, like CPR, cycles between the one-electron- and three-electron-reduced states (*26*). Furthermore, analysis of the flavin midpoint potentials and the removal of the FMN cofactor suggest that the path of electron transfer in both enzymes is from NADPH to FAD to FMN to the heme (*20*, *27*−*30*).

NOS and CPR are also able to reduce 2,6-dichloroindolphenol (DCIP), ferricyanide (FeCN), and cytochrome c^{3+} with electrons derived from NADPH oxidation (*31*, *32*). However, nNOS is unique in that the binding of Ca^{2+}-CaM to the enzyme stimulates a 2−3-fold increase in the levels of DCIP and FeCN reduction and a 10−20-fold increase in the level of cytochrome c^{3+} reduction (*10*, *18*). The Ca^{2+}-CaM-induced stimulation of these activities is independent of electron transfer from the flavins to the heme since the same level of stimulation of ferricyanide and cytochrome c^{3+} reduction occurs with nNOS devoid of its oxygenase domain (*18*, *26*, *33*). Stopped-flow studies have indicated that the binding of Ca^{2+}-CaM increases the pre-steady-state rate of electron transfer from NADPH to the flavins (*18*, *34*). The binding of Ca^{2+}-CaM has a negligible effect on the flavin redox potentials, indicating that the thermodynamic driving force of electron transfer remains unchanged (*28*). However, the increase in the rate of electron transfer may be facilitated by the ability of Ca^{2+}-CaM to induce a conformational change in the enzyme (*10*, *26*).

The reductase domain of NOS also has additional amino acid sequences that are not found in CPR. nNOS and eNOS, which have slower rates of electron transfer to the heme, DCIP, and cytochrome c^{3+}, contain an additional 40−50-amino acid insert located in the FMN-binding subdomain. This insert is thought to be an autoinhibitory domain since it was shown to promote the dissociation of CaM from nNOS at low intracellular Ca^{2+} concentrations and to inhibit electron transfer in the absence of Ca^{2+}-CaM (*30*, *35*, *36*). Both iNOS and the constitutive isoforms possess an additional 21−42-amino acid tail at the C-terminus, which is not present in CPR. This sequence is proposed to modulate electron transfer between the flavin moieties or between FMN and cytochrome c^{3+} (*37*).

When the additional structural and dynamic features in NOS that are absent in CPR are considered, there is interest in how Ca^{2+}-CaM imparts control of electron transfer. Although several pre-steady-state kinetic and mutational analyses have been performed to investigate the effects of Ca^{2+}-CaM on interflavin electron transfer, the influence of the cofactor on the kinetic mechanism of electron transfer within the reductase domain of the enzyme remains to be elucidated. Establishing a mechanism is important for studying the overall rate of NO production since the control point of electron transfer resides within the reductase domain of the enzyme. This is suggested by the different rates of NO synthesis exhibited by the three isoforms as determined by the rate of electron transfer between FAD and FMN or between FMN and the heme (*38*). The data presented below describe the steady-state kinetic mechanism of the NOS-catalyzed electron transfer to cytochrome c^{3+} and DCIP in the presence and absence of Ca^{2+}-CaM. We chose to investigate these two electron acceptors since DCIP is reduced by a two-electron transfer from reduced FAD and is stimulated only 2−3-fold by Ca^{2+}-CaM (*29*). In contrast, cytochrome c^{3+} is reduced by donation of one electron from FMN and the binding of Ca^{2+}-CaM causes a 10−20-fold increase in activity. Initial velocity and product inhibition data for the nNOS-catalyzed reduction of DCIP were consistent with an iso ping-pong bi-bi mechanism, with a steady-state isomerization step between the release of $NADP^+$ and the binding of DCIP. In contrast, initial velocity and product inhibition data for the reduction of cytochrome c^{3+} were best accommodated by a nonclassical (two-site) ping-pong mechanism. However, dead-end inhibition studies revealed a large difference in the K_{is} values of 2′AMP in competitive inhibition patterns versus NADPH for DCIP compared to cytochrome c^{3+}. To rationalize the difference in the K_{is}, value an additional rapidly equilibrating isomerization step between the enzyme form found immediately after the release of the last product (E_1′) and the enzyme form competent to bind NADPH (E_1) was required in both mechanisms (E_1′ binds 2′AMP, but not NADPH, while E_1 does not bind 2′AMP). The rate equations describing DCIP and cytochrome c^{3+} reduction were derived for a di-iso ping-pong bi-bi and an iso (two-site) ping-pong mechanism, respectively. The presence of Ca^{2+}-CaM did not alter the observed steady-state kinetic mechanisms proposed for the reduction of DCIP and cytochrome c^{3+}. Ca^{2+}-CaM did affect to varying degrees the kinetic parameters for the substrates NADPH, cytochrome c^{3+}, and DCIP.

EXPERIMENTAL PROCEDURES

Materials. The cDNA for rat neuronal NOS was kindly provided by T. M. Dawson (Johns Hopkins University, Baltimore, MD) (*39*), and the pCWori expression vector was a gift of F. W. Dalhquist (University of Oregon, Eugene, OR) (*40*). Tetrahydrobiopterin (H_4B) was purchased from Cayman Chemical (Ann Arbor, MI); the 2′,5′-ADP-Sepharose was purchased from Amersham Pharmacia Biotech (Piscataway, NJ), and the CaM-Sepharose and CaM were generous gifts of S. Anderson and D. Malencik (Oregon State University). All other reagents were from Sigma Chemical Co. (St. Louis, MO).

Enzyme Expression and Purification. The enzyme was purified according to the protocol published by Gerber and Ortiz de Montellano with slight modification (*41*). The recombinant purified protein was more than 85% pure as judged by SDS−polyacrylamide gel electrophoresis with a specific activity of 150 nmol of NO min^{-1} mg^{-1} at 25 °C. The rate of NO production was measured by the hemoglobin−NO capture assay following the procedures of Stuehr et al. (*42*). Protein concentrations were determined with the Lowry assay using BSA as a standard (*43*).

Measurement of Reductase Activities. Reactions were performed in a volume of 5.0 mL at 25 °C using either a 10 or 5 cm path length cuvette. The reaction rate was measured by reduction of cytochrome c^{3+} ($\Delta\epsilon = 21.1$ mM^{-1} cm^{-1}) at 550 nm or DCIP ($\Delta\epsilon = 21$ mM^{-1} cm^{-1}) at 600 nm (*44*). Reaction mixtures contained 50 mM Hepes (pH 7.5), variable concentrations of substrates (NADPH, cytochrome c^{3+}, or DCIP), and, where appropriate, 10 μM $CaCl_2$, 100 nM CaM, and variable concentrations of inhibitor ($NADP^+$, 2′AMP, or cytochrome c^{2+}). Reactions were initiated in a total volume of 5 mL by the addition of 0.08−0.8 μg of nNOS.

Preparation of Cytochrome c^{2+}. Cytochrome c^{2+} was prepared by reducing cytochrome c^{3+} with sodium dithionite. After incubation for 10 min at room temperature, the sodium dithionite was removed by passing 1 mL of the solution over two columns (2 mL) of G-25 resin. The concentration of cytochrome c^{2+} was determined by measuring the absorbance at 550 nm before and after reduction with sodium dithionite using the extinction coefficients for reduced ($\epsilon = 29.5$ mM^{-1} cm^{-1}) and oxidized ($\epsilon = 8.4$ mM^{-1} cm^{-1}) cytochrome *c* (*44*).

Data Analysis. Data were first analyzed graphically using primary plots of reciprocal velocities and reciprocal substrate concentrations. Slopes and intercepts obtained from the primary plots were then graphed as secondary plots versus inhibitor concentrations. The form of the overall rate equation was determined by examination of the results of the graphical analysis. Although the kinetic results are presented in double-reciprocal plots, the computer analysis was performed by the nonlinear least-squares fit to the specific rate equation using the computer program Origin, version 4.0 (MicroCal Software Inc., North Hampton, MA). The data from initial velocity studies were fit to eq 1 for a ping-pong mechanism and to eq 2 for a sequential mechanism.

$$v_i = \frac{VAB}{K_B A + K_A B + AB} \quad (1)$$

$$v_i = \frac{VAB}{K_{iA} K_B + K_B A + K_A B + AB} \quad (2)$$

where v_i is the initial velocity, A and B are concentrations of NADPH and the electron acceptor (cytochrome c^{3+} or DCIP), respectively, V is the maximal velocity, K_A and K_B are the Michaelis constants for A and B, respectively, and K_{iA} is the dissociation constant for NADPH. Data from inhibition studies were fit to equations for competitive (eq 3), uncompetitive (eq 4), and noncompetitive (eq 5) inhibition:

$$v_i = \frac{VA}{K_m(1 + I/K_{is}) + A} \quad (3)$$

$$v_i = \frac{VA}{K_m + A(1 + I/K_{ii})} \quad (4)$$

$$v_i = \frac{VA}{K_m(1 + I/K_{is}) + A(1 + I/K_{ii})} \quad (5)$$

where v_i is the initial velocity, V is the maximal velocity, A is the varied substrate concentration, K_m is the apparent Michaelis constant, I is the inhibitor concentration, K_{ii} is the intercept inhibition constant, and K_{is} is the slope inhibition constant. For all reactions, the nonvaried substrate was present at a level close to its K_m.

RESULTS

Initial Velocity Studies with DCIP as an Electron Acceptor. Substrate inhibition by NADPH for DCIP reduction occurred at concentrations of NADPH 2-fold above its K_m. Substrate inhibition by NADPH is also observed for the FAD-containing enzyme, nitrate reductase (*45*). Therefore, the concentration of NADPH with DCIP as an electron acceptor was varied between $K_m/5$ and K_m for the initial velocity experiments. A plot of $1/v_i$ versus 1/[DCIP] at varying fixed concentrations of NADPH showed a family of parallel lines in the absence of Ca^{2+}-CaM (Figure 1A) and in the presence Ca^{2+}-CaM (Figure 1B). Similarly, a plot of $1/v_i$ versus 1/[NADPH] at varying fixed concentrations of DCIP showed a family of parallel lines in the absence and presence of Ca^{2+}-CaM (panels C and D of Figure 1, respectively). A parallel pattern is typical of ping-pong mechanisms in which an irreversible step such as release of a product or the addition of substrate at saturating levels separates the addition of either of the two substrates in the reaction sequence (*46*). A better nonlinear least-squares fit of the initial velocity data was achieved with the equation describing a ping-pong mechanism (eq 1) compared to that for a sequential mechanism (eq 2). The latter equation did not reduce the χ^2 value and gave an undefined value for K_{iA}.

Ping-pong mechanisms are characterized by the enzyme oscillating between two or more stable forms (*47*). As illustrated in Scheme 1, the air-stable one-electron-reduced state of nNOS, E_1, is designated as one of these stable enzyme forms. The oxidation of one NADPH molecule generates the second stable enzyme form, the three-electron-reduced state of nNOS, E_3. Since DCIP reduction is a two-electron process, only one molecule is required to react with E_3 in the subsequent half-reaction to return the enzyme to E_1. If DCIP reduction were to follow this classical ping-pong mechanism, the substrates and products would bind to the enzyme in a tetra-uni fashion.

The presence of Ca^{2+}-CaM resulted in a 3-fold increase in k_{cat}, a 4.5-fold increase in $(k_{cat}/K_m)_{DCIP}$, and a 1.5-fold increase in $(k_{cat}/K_m)_{NADPH}$ (Table 1). The experimentally determined Michaelis constants for NADPH (*48*, *49*) and DCIP and the turnover number (k_{cat}) for DCIP reduction with and without Ca^{2+}-CaM agree with previously reported values (*31*).

Product Inhibition Studies with DCIP as an Electron Acceptor. As indicated in Table 2, $NADP^+$ was noncompetitive with either NADPH or DCIP as the variable substrate, and the dead-end inhibitor, 2′AMP, was competitive versus NADPH and uncompetitive versus DCIP. The inhibition patterns are consistent with the classical ping-pong mechanism illustrated in Scheme 1 with one exception. Product inhibition by $NADP^+$ is expected to be competitive versus DCIP, because they both bind to the same enzyme form, E_3 (*47*). However, $NADP^+$ was noncompetitive versus DCIP, indicating that they bind to different forms of E_3. The kinetic mechanism was therefore revised to incorporate a step which allows E_3 to isomerize to a distinct three-electron-reduced state, E_3', which exclusively binds DCIP (Scheme 2). When an isomerization of a stable form of the enzyme occurs in the reaction sequence, it is termed an iso mechanism (*47*). To follow previously established nomenclature, the mechanism is drawn in Scheme 2 is termed an iso ping-pong bi-bi type (*47*).

Saturating levels of Ca^{2+}-CaM in the reaction mixtures did not affect the product and dead-end inhibition patterns. It did increase the K_{is} for 2′AMP versus NADPH 2-fold, but did not affect the K_{ii} for 2′AMP with DCIP as the variable substrate (Table 2).

Initial Velocity Studies with Cytochrome c^{3+} as an Electron Acceptor. Cytochrome c^{3+} shows substrate inhibition at concentrations of >2 μM (5−10 times its K_m); therefore, this electron acceptor was maintained at sufficiently low

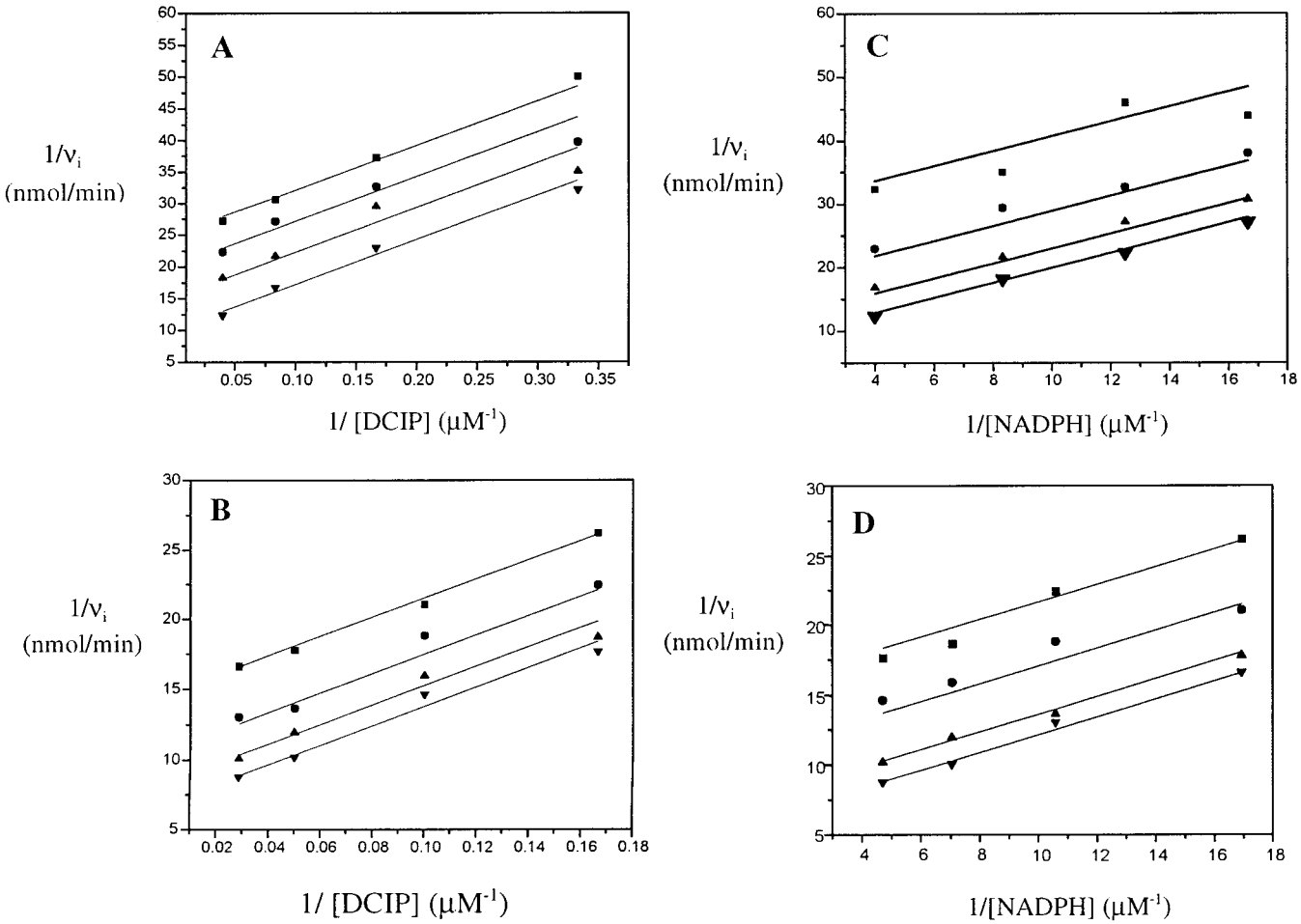

FIGURE 1: Initial velocity patterns for the nNOS-catalyzed reduction of DCIP by NADPH. The symbols represent the experimentally determined means of three values, while the lines are best nonlinear fits to the data. (A) Varying concentrations of DCIP at NADPH concentrations of (■) 0.05, (●) 0.08, (▲) 0.12, and (▼) 0.25 μM. (B) $CaCl_2$ at 10 μM and CaM at 100 nM present with varying concentrations of DCIP at NADPH concentrations of (■) 0.059, (●) 0.094, (▲) 0.142, and (▼) 0.213 μM. (C) Varying concentrations of NADPH at DCIP concentrations of (■) 3, (●) 6, (▲) 12, and (▼) 25 μM. (D) $CaCl_2$ at 10 μM and CaM at 100 nM present with varying concentrations of NADPH at DCIP concentrations of (■) 6, (●) 10, (▲) 20, and (▼) 35 μM.

Scheme 1

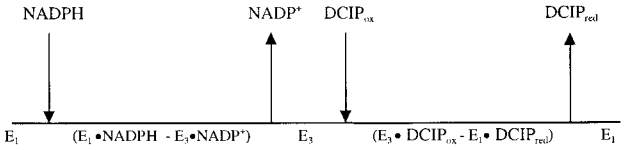

concentrations to minimize this effect. Substrate inhibition by cytochrome c^{3+} also occurs with CPR at 5−10 times its K_m (*50*). A plot of $1/v$ versus 1/[cytochrome c^{3+}] at varying fixed concentrations of NADPH gave a family of parallel lines both without Ca^{2+}-CaM (Figure 2A) and with Ca^{2+}-CaM (Figure 2B). Likewise, a plot of $1/v$ versus 1/[NADPH] at varying fixed concentrations of cytochrome c^{3+} in the absence and presence of Ca^{2+}-CaM produced a family of parallel lines (panels C and D of Figure 2, respectively). The lack of a slope effect suggests that both basal and CaM-stimulated cytochrome c^{3+} reductase activities are consistent with ping-pong mechanisms. This graphical analysis is consistent with the computer analysis as the rate equation for a ping-pong mechanism (eq 1) gave a better fit to the initial velocity data compared to the rate equation for a sequential mechanism (eq 2). The latter equation did not reduce the χ^2 value and gave an undefined value for K_{iA}.

If the nNOS reduction of cytochrome c^{3+} were to follow the classical ping-pong mechanism, the binding of substrates and release of products would proceed in a hexa-uni fashion (Scheme 3) (*50*). After the initial conversion of E_1 to E_3 by NADPH oxidation, two molecules of cytochrome c^{3+}, each of which is reduced by one electron, are required to react with the enzyme to return it to its initial state, E_1 (Scheme 3). Thus, the two-electron-reduced state, E_2, now appears after the reduction of the first molecule of cytochrome c^{3+}. Equation 1 is also consistent with a nonclassical (two-site) ping-pong mechanism (*50*). In this kinetic mechanism, NADPH and cytochrome c^{3+} react at two catalytically independent sites on the enzyme. Scheme 4 illustrates the (two-site) ping-pong mechanism with the active sites for NADPH and cytochrome c^{3+} labeled as sites 1 and 2, respectively. This mechanism has been previously proposed for the CPR-catalyzed reduction of cytochrome c^{3+}. When the structural and functional similarities of nNOS and CPR are considered, it seems reasonable that this mechanism also applies for the nNOS cytochrome c^{3+} reductase activity. The classical (one site) and the nonclassical (two-site) mechanisms drawn in Schemes 3 and 4, respectively, generate different product and dead-end inhibition patterns (*50, 51*); therefore, there is a means for discerning which mechanism

Table 1: Values for the Steady-State Kinetic Parameters of nNOS-Catalyzed Reduction of DCIP and Cytochrome c^{3+} in the Absence and Presence of Ca^{2+}-CaM

electron acceptor	Ca^{2+}-CaM	K_{NADPH}[a,e] (μM)	K_{acc}[b,e] (μM)	k_{cat}[c,e] (s^{-1})	k_{cat}[d]/K_{NADPH} ($\times 10^5$ M^{-1} s^{-1})	k_{cat}[d]/K_{acc} ($\times 10^5$ M^{-1} s^{-1})
DCIP	−	0.18 ± 0.05 (5)	15.9 ± 1.9 (3)	5.41 ± 0.35 (5)	300.7 ± 85.7	3.43 ± 0.47
	+	0.35 ± 0.05 (5)	10.3 ± 1.7 (3)	16.10 ± 0.52 (5)	460.0 ± 67.3	15.63 ± 1.18
cytc	−	0.02 ± 0.01 (6)	0.4 ± 0.1 (11)	1.64 ± 0.05 (5)	725.7 ± 261.7	43.17 ± 11.3
	+	0.25 ± 0.09 (5)	0.4 ± 0.1 (4)	37.16 ± 0.91 (5)	1486 ± 536	1004 ± 272

[a] K_{NADPH} is the Michaelis constant for NADPH. [b] K_{acc} is the Michaelis constant for the designated electron acceptor. [c] k_{cat} is the maximal velocity, V, divided by the nNOS concentration. [d] k_{cat}/K_{NADPH} and k_{cat}/K_{acc} are V/K_{NADPH} and V/K_{acc} divided by the nNOS concentration, respectively. [e] The values are the means and standard deviations determined from n determinations where n is enclosed in parentheses.

Table 2: Dead-End and Product Inhibition of nNOS-Catalyzed Reduction of DCIP in the Absence and Presence of Ca^{2+}-CaM

varied substrate	Ca^{2+}-CaM	inhibitor	type of inhibition	inhibition constants (μM)
DCIP	−	$NADP^+$	noncompetitive	$K_{is} = 8.1 \pm 1.8$ $K_{ii} = 13.0 \pm 2.0$
	+	$NADP^+$	noncompetitive	$K_{is} = 18.6 \pm 5.2$ $K_{ii} = 12.2 \pm 5.2$
	−	2′AMP	uncompetitive	$K_{ii} = 435.4 \pm 23.1$
	+	2′AMP	uncompetitive	$K_{ii} = 435.6 \pm 34.0$
NADPH	−	$NADP^+$	noncompetitive	$K_{is} = 14.5 \pm 1.5$ $K_{is} = 27.7 \pm 1.8$
	+	$NADP^+$	noncompetitive	$K_{is} = 8.1 \pm 1.4$ $K_{ii} = 58.9 \pm 12.0$
	−	2′AMP	competitive	$K_{is} = 840.9 \pm 92.9$
	+	2′AMP	competitive	$K_{is} = 1437.0 \pm 280.8$

Scheme 2

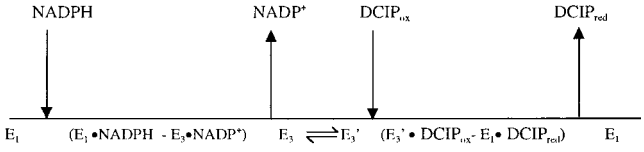

applies for the nNOS reduction of cytochrome c^{3+}.

The presence of Ca^{2+}-CaM did not alter the parallel pattern of the double-reciprocal plots (panels B and D of Figure 2); however, the presence of the activated cofactor resulted in a 23-fold increase in k_{cat} and $(k_{cat}/K_m)_{cytc}$ (Table 1). The average value of $(k_{cat}/K_m)_{NADPH}$ increased 2-fold with the addition of Ca^{2+}-CaM; however, due to the large errors associated with the values, the change was not considered significant (Table 1).

Product Inhibition Studies with Cytochrome c^{3+} as an Electron Acceptor. Although the parallel initial velocity patterns with cytochrome c^{3+} as the terminal electron acceptor are consistent with either a classical (one-site) ping-pong mechanism (Scheme 3) or a nonclassical (two-site) ping-pong mechanism (Scheme 4), product and dead-end inhibition patterns are consistent only with the latter of these two kinetic mechanisms. The results of the inhibition studies, summarized in Table 3, show that product inhibition by $NADP^+$ was competitive versus NADPH and that by cytochrome c^{2+} was competitive versus cytochrome c^{3+}. These patterns are consistent with the (two-site) ping-pong mechanism (*50*) (Appendix). In the classical (one-site) hexa-uni ping-pong mechanism drawn in Scheme 3, both of these inhibition patterns are expected to be noncompetitive; therefore, this mechanism is not consistent for the nNOS reduction of cytochrome c^{3+} (Appendix). The remaining inhibition patterns listed in Table 3 are consistent with the (two-site) ping-pong mechanism since product inhibition by $NADP^+$ was found to be uncompetitive versus cytochrome c^{3+} and cytochrome c^{2+} was found to be a noncompetitive product inhibitor versus NADPH. Finally, the dead-end inhibition by the NADPH analogue, 2′AMP, was competitive with NADPH as the variable substrate and uncompetitive with cytochrome c^{3+} as the variable substrate.

The presence of Ca^{2+}-CaM did not affect the product and the dead-end inhibition patterns. However, a saturating amount of Ca^{2+}-CaM in the reaction mixture increased the value of K_{is} by 1.5−2.5-fold for both $NADP^+$ and 2′AMP with NADPH as the variable substrate. The K_{ii} for 2′AMP inhibition versus cytochrome c^{3+} or DCIP did not change significantly in the presence of Ca^{2+}-CaM. However, the K_{ii} for $NADP^+$ decreased approximately 4-fold in inhibition studies with varying concentrations of cytochrome c^{3+}.

Dead-End Inhibition by 2′AMP. The K_{is} for 2′AMP in inhibition studies with NADPH as the variable substrate decreased 25−30-fold when the electron acceptor was changed from DCIP to cytochrome c^{3+} (Tables 2 and 3). Furthermore, the K_{ii} for 2′AMP was 4−5-fold higher when DCIP rather then cytochrome c^{3+} was the variable substrate. Both K_{ii} and K_{is} values for the NADPH analogue changed by similar amounts under the same conditions with Ca^{2+}-CaM. In the kinetic mechanisms proposed for DCIP (Scheme 2) and cytochrome c^{3+} (Scheme 4), 2′AMP is expected to bind to the same enzyme form as NADPH, E_1. This would accommodate both competitive and uncompetitive patterns for 2′AMP versus NADPH and versus the electron acceptor, respectively. If this were the case, both of the apparent affinity constants for 2′AMP should be the same regardless of the electron acceptor, because the dead-end inhibitor is binding to a substrate-free form of the enzyme, E_1, in both mechanisms. To explain the observed differences in the apparent affinity for 2′AMP, a second form of E_1, labeled E_1′ in Figures 3 and 4, which is able bind 2′AMP but not NADPH, is proposed to exist in both kinetic mechanisms. To satisfy the competitive dead-end inhibition patterns versus NADPH, the isomerization of E_1′ to E_1 must be in rapid equilibrium. If this step were at steady state, 2′AMP would be noncompetitive versus NADPH. The kinetic mechanism for the reduction of DCIP was modified and renamed to include this second, faster isomerization step and is now termed a di-iso ping-pong bi-bi mechanism. Likewise, the reduction of cytochrome c^{3+} is now proposed to follow an iso (two-site) ping-pong mechanism.

DISCUSSION

The classical method for distinguishing between sequential and ping-pong reaction mechanisms is by analysis of the initial velocity patterns obtained by varying the concentration

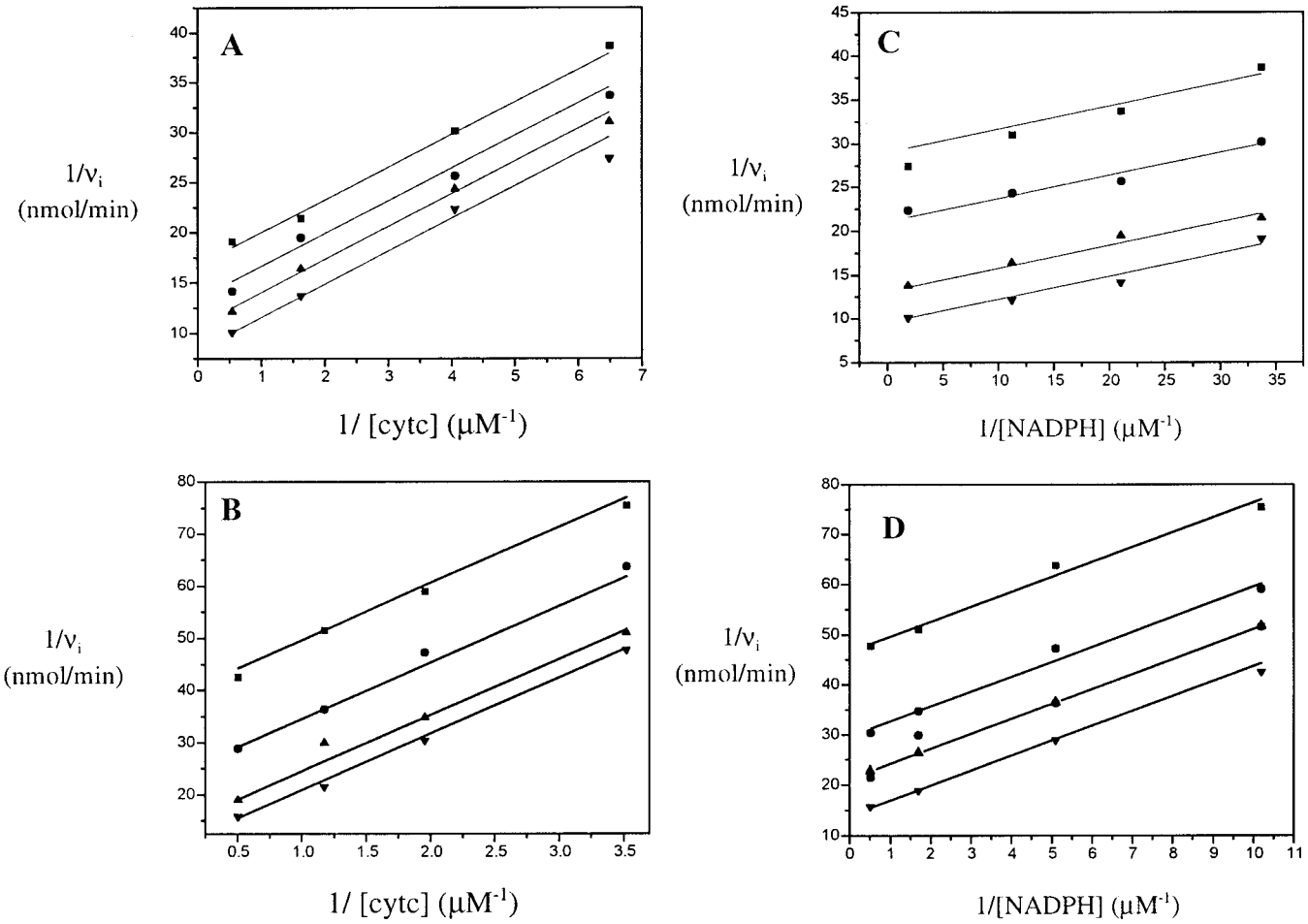

FIGURE 2: Initial velocity patterns for the nNOS-catalyzed reduction of cytochrome c^{3+} by NADPH. The symbols represent the experimentally determined mean of three values, while the lines are best nonlinear fits to the data. (A) Varying concentrations of cytochrome c^{3+} (cytc) at NADPH concentrations of (■) 0.029, (●) 0.047, (▲) 0.089, and (▼) 0.534 μM. (B) $CaCl_2$ at 10 μM and CaM at 100 nM present with varying concentrations of cytochrome c^{3+} at NADPH concentrations of (■) 0.098, (●) 0.196, (▲) 0.588, and (▼) 1.96 μM. (C) Varying concentrations of NADPH at cytochrome c^{3+} concentrations of (■) 0.154, (●) 0.246, (▲) 0.619, and (▼) 1.848 μM. (D) $CaCl_2$ at 10 μM and CaM at 100 nM present with varying concentrations of NADPH at cytochrome c^{3+} concentrations of (■) 0.28, (●) 0.51, (▲) 0.85, and (▼) 1.99 μM.

Scheme 3

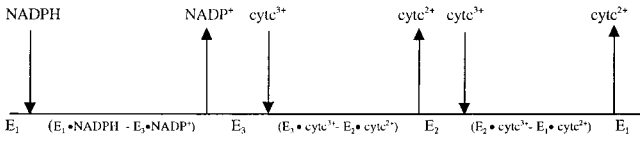

Scheme 4

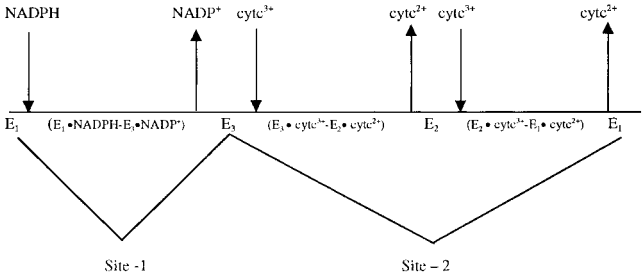

Table 3: Dead-End and Product Inhibition of nNOS-Catalyzed Reduction of Cytochrome c^{3+} in the Absence and Presence of Ca^{2+}-CaM

varied substrate	Ca^{2+}-CaM	inhibitor	type of inhibition	inhibition constants (μM)
$cytc^{3+}$	−	$cytc^{2+}$	competitive	$K_{is} = 2.3 \pm 0.3$
	+	$cytc^{2+}$	competitive	$K_{is} = 4.1 \pm 0.4$
	−	$NADP^+$	uncompetitive	$K_{ii} = 6.2 \pm 0.5$
	+	$NADP^+$	uncompetitive	$K_{ii} = 1.6 \pm 0.1$
	−	2′AMP	uncompetitive	$K_{ii} = 95.3 \pm 2.7$
	+	2′AMP	uncompetitive	$K_{ii} = 82.4 \pm 2.3$
NADPH	−	$cytc^{2+}$	noncompetitive	$K_{is} = 6.1 \pm 1.1$ $K_{ii} = 2.3 \pm 1.0$
	+	$cytc^{2+}$	noncompetive	$K_{is} = 7.1 \pm 1.0$ $K_{ii} = 9.6 \pm 0.7$
	−	$NADP^+$	competitive	$K_{is} = 1.2 \pm 0.1$
	+	$NADP^+$	competitive	$K_{is} = 2.1 \pm 0.1$
	−	2′AMP	competitive	$K_{is} = 31.5 \pm 2.9$
	+	2′AMP	competitive	$K_{is} = 71.5 \pm 3.8$

of one substrate at several fixed concentrations of a second substrate. When the data are plotted in double-reciprocal form, ping-pong mechanisms give patterns of parallel lines while sequential mechanisms will yield a family of lines which intersect to the left of the vertical axis (*52*). The initial velocity experiments with DCIP and cytochrome c^{3+} in the presence and absence of Ca^{2+}-CaM fit best to eq 1 for a ping-pong mechanism. Abu-Soud et al. (*53*, *54*) have shown that the flavin cofactors of nNOS can be reduced with the addition of excess NADPH in the absence of any electron acceptor. These data support the ping-pong mechanism, because it demonstrates that a binary complex between nNOS

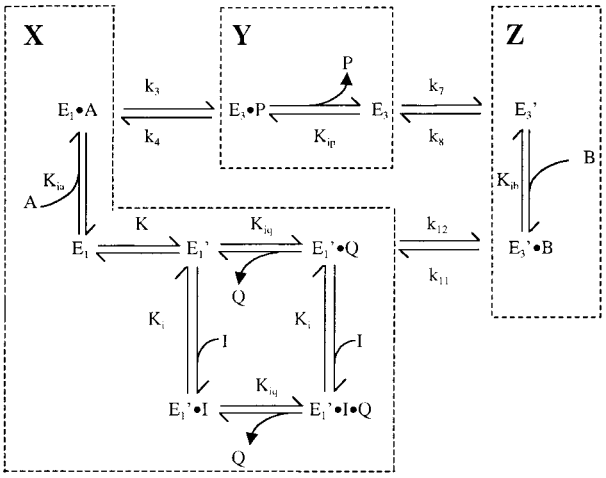

FIGURE 3: Kinetic scheme for a di-iso ping-pong bi-bi mechanism for the nNOS-catalyzed reduction of DCIP. A, B, P, Q, and I represent NADPH, $DCIP_{ox}$, $NADP^+$, $DCIP_{red}$, and 2′AMP, respectively, and the K_i values refer to their respective dissociation constants. E_1 and E_1' are the one-electron (FAD-$FMNH^\bullet$) forms of nNOS that exclusively bind NADPH and 2′AMP, respectively. E_3 and E_3' are the three-electron ($FADH^\bullet$-$FMNH_2$) or ($FADH_2$-$FMNH^\bullet$) forms of nNOS that exclusively bind $NADP^+$ and $DCIP_{ox}$, respectively. K is the equilibrium constant for the conversion of the two enzyme forms, E_1 and E_1'. The dotted boxes labeled X, Y, and Z indicate the proposed rapid equilibrium segments for the reaction mechanism, where $X = E_1 + E_1' + E_1'I + E_1'IQ + E_1'Q + E_1A$, $Y = E_3P + E_3$, and $Z = E_3' + E_3'B$.

Site-1:

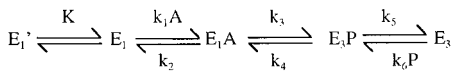

Site-2:

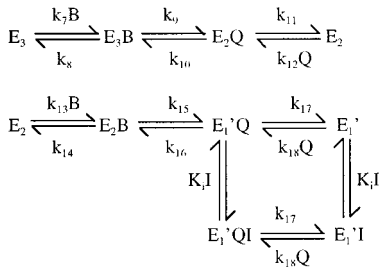

FIGURE 4: Kinetic scheme illustrating the iso (two-site) ping-pong mechanism for the nNOS-catalyzed reduction of cytochrome c^{3+}. A, B, P, Q, and I represent NADPH, cytochrome c^{3+}, $NADP^+$, cytochrome c^{2+}, and 2′AMP, respectively. E_1, E_1,′ and E_3 are the same as in Figure 3, and E_2 represents the two-electron-reduced form of nNOS (FAD-$FMNH_2$).

and either electron acceptor is not a prerequisite for the binding and subsequent oxidation of NADPH.

Although nNOS maintains one electron on its flavins in the form of a flavin semiquinone (FAD-$FMNH^\bullet$), it is unable to transfer this electron to either DCIP or cytochrome c^{3+} (*23*). This one-electron-reduced state of nNOS, E_1, is then postulated to be one of the stable enzyme forms in the ping-pong mechanisms for DCIP and cytochrome c^{3+}. Since hydride transfer from NADPH results in the transfer of two electrons to the flavins, the three-electron-reduced state, E_3, is thought to be the second stable enzyme form in the reaction sequences for both electron acceptors. However, the kinetic mechanisms for DCIP and cytochrome c^{3+} differ once the number of electrons required to reduce the electron acceptor is considered. The reduction of DCIP is a two-electron process; therefore, one molecule combining with E_3 is enough to return the enzyme to E_1. Scheme 1 illustrates the tetra-uni ping-pong mechanism for the reduction of this substrate. In contrast, cytochrome c^{3+} is reduced by one electron; therefore, it would follow a hexa-uni ping-pong mechanism, which would include the formation of E_2 after the reduction of the first molecule of cytochrome c^{3+} (Scheme 3).

The kinetic mechanisms for the reduction of DCIP and cytochrome c^{3+} illustrated in Schemes 1 and 3, respectively, are modified to be consistent with the product and dead-end inhibition studies in Tables 2 and 3. The kinetic mechanism for DCIP reduction was revised to incorporate an iso step, or an isomerization of E_3 to E_3' (Scheme 2), based on the noncompetitive inhibition by $NADP^+$ at varying concentrations of DCIP. According to the classical ping-pong mechanism depicted in Scheme 1, $NADP^+$ and DCIP combine with the same enzyme form, E_3; therefore, $NADP^+$ is expected to be competitive versus DCIP. However, if the two molecules bind exclusively to different conformations of E_3 or to alternate forms of E_3 that arise from differences in the distribution of the three electrons on the flavins [i.e., ($FADH^\bullet$-$FMNH_2$) versus ($FADH_2$-$FMNH^\bullet$)], and the rate of isomerization between the two forms is at steady state, noncompetitive inhibition is expected. Thus, this iso step is not included in either rapid equilibrium segment Y or Z of Figure 3. If the iso step were to occur in rapid equilibrium, $NADP^+$ would be a competitive inhibitor when DCIP is the variable substrate. The noncompetitive inhibition of $NADP^+$ when NADPH is the variable substrate (Table 2) is consistent with the proposed mechanism in Scheme 2 since the reduced and oxidized forms of the nucleotide bind to E_1 and E_3, respectively. Dead-end inhibition patterns with the NADPH analogue, 2′AMP, are also consistent with the proposed kinetic mechanism. The dead-end inhibitor was found to be competitive versus NADPH, which is consistent with them both binding to the same enzyme form. The NADPH analogue was also found to be uncompetitive versus DCIP (Table 2), which is consistent with binding to different enzyme forms connected by an irreversible step, the release of $NADP^+$.

The parallel initial velocity patterns observed with cytochrome c^{3+} as an electron acceptor agree with both the classical (one-site) ping-pong mechanism (Scheme 2) and the (two-site) ping-pong mechanism (Scheme 4) (*46*). However, product and dead-end inhibition studies are consistent only with the latter of these two kinetic mechanisms. The defining characteristic of the (two-site) ping-pong mechanism is presence of two separate and functionally distinct catalytic sites on the enzyme that are linked by a mobile component or by an internal electron carrier. This type of system was first used to describe enzymes that contain a mobile component, such as a biotinyl prosthetic group (*51*, *55*) or lipoic acid cofactor (*56*), which links the nonoverlapping catalytic sites on the enzyme. It has also been shown to be applicable for enzymes with redox cofactors that serve as internal electron carriers, such as xanthine dehydrogenase (*57*), glutamate synthetase (*58*), nitrate reductase (*45*), two hydrogenases (*59*, *60*), and dihydroorate dehydrogenase (*61*). The two-site ping-pong mechanism is also proposed for the CPR-catalyzed reduction of cytochrome

c^{3+} in which the FAD/FMN prosthetic groups act as internal electron carriers between the NADPH and the cytochrome c^{3+} active sites. When the functional and structural homology between CPR and the nNOS reductase domain is considered, it seems reasonable that the product and dead-end inhibition studies for the nNOS-catalyzed reduction of cytochrome c^{3+} are also consistent with a (two-site) ping-pong mechanism. In this mechanism, the product ($NADP^+$ or cytochrome c^{2+}) can be released before or after the addition of the substrate (NADPH or cytochrome c^{3+}) and the reaction is not restricted to either exclusive formation of binary complexes or compulsory formation of a central ternary complex.

This is in contrast to the classical (one-site) hexa-uni ping-pong mechanism shown in Scheme 3 where the formation of the ternary complex is precluded. With this mechanism, product inhibition by $NADP^+$ is expected to be noncompetitive versus NADPH and competitive versus cytochrome c^{3+} (Appendix). Furthermore, product inhibition by cytochrome c^{2+} is expected to be noncompetitive versus NADPH and noncompetitive versus cytochrome c^{3+} (Appendix). Instead, $NADP^+$ was found to be a competitive inhibitor when NADPH was the variable substrate and an uncompetitive inhibitor versus cytochrome c^{3+}. Cytochrome c^{2+} was noncompetitive versus NADPH and competitive when cytochrome c^{3+} was the variable substrate (Table 3). These patterns are identical with those reported for the CPR-catalyzed reduction of cytochrome c^{3+} (*50*) and are consistent with the unique product inhibition patterns that are commonly observed with the enzymes listed above which follow a (two-site) ping-pong mechanism. The first product (P) is always competitive with the first substrate (A). Similarly, inhibition by the second product (Q) is competitive with the second substrate (B) (*45*). Therefore, we propose that the nNOS-catalyzed reduction of cytochrome c^{3+} also follows a (two-site) ping-pong mechanism in which the enzyme binds NADPH at site 1 in a uni-uni fashion and follows a tetra-uni ping-pong reaction for two molecules of cytochrome c^{3+} at site 2 (Scheme 4). This kinetic mechanism is only applicable for CPR at a high ionic strength, 850 mM (*50*). At a lower ionic strength (300 mM), the CPR cytochrome c^{3+} reductase activity is still consistent with a (two-site) ping-pong mechanism, but the binding of cytochrome c^{3+} follows a bi-bi random sequential mechanism at site 2 (*62*). This was deduced from the nonlinear initial velocity patterns observed when cytochrome c^{3+} was the variable substrate for CPR at low ionic strengths. However, nNOS does not show any curvature in the initial velocity patterns for reduction of cytochrome c^{3+} at low ionic strengths (panels A and B of Figure 2).

Inhibition by $NADP^+$ versus cytochrome c^{3+} at nonsaturating concentrations of NADPH should be noncompetitive for a two-site ping-pong mechanism, but CPR and nNOS both exhibited uncompetitive inhibition patterns (Table 3). To explain this observation, it was assumed that the reverse rate of hydride transfer, k_4, catalyzed by CPR was much slower than the rate of cytochrome c^{3+} reduction, k_9 (Figure 4) (*50*). The lack of any pronounced curvature in inhibition patterns with cytochrome c^{2+} further indicated that hydride transfer, k_3, was much slower than electron transfer from the flavins to cytochrome c^{3+}, k_9 (*50*). Since nNOS exhibits the same inhibition patterns as CPR and it does not display any curvature in the inhibition patterns with cytochrome c^{2+} (data not shown), this assumption ($k_9 \gg k_4$) was also used in the derivation of the (two-site) ping-pong mechanism for nNOS-catalyzed reduction of cytochrome c^{3+} (Appendix).

In the one-site ping-pong mechanism for DCIP, only binary enzyme−substrate complexes form and the release of the first product, $NADP^+$, occurs before the addition of DCIP. However, since NADPH and cytochrome c^{3+} are proposed to act at catalytically independent sites on the enzyme, the formation of a ternary complex between the two substrates and nNOS is possible. The difference may be do to the flavin cofactor that reduces the electron acceptor. Since nNOS depleted of its FMN cofactor is still able to reduce DCIP, the reduction of this substrate may occur through the direct two-electron transfer from the fully reduced FAD, presumably through the conversion of ($FADH_2$-$FMNH^\bullet$) to (FAD-$FMNH^\bullet$) (*29*). Once NADPH reduces E_1 (FAD-$FMNH^\bullet$) to E_3, disproportionation of electrons on the flavins establishes an equilibrium of ($FADH_2$-$FMNH^\bullet$) and ($FADH^\bullet$-$FMNH_2$). It has been proposed that $NADP^+$ shifts the reduction potential of the FAD semiquinone to a more negative value and stabilizes the $FADH^\bullet$-$FMNH_2$ form of the enzyme (*28*). Similar effects have been observed in P450-BM3 (*63*) and adrenodoxin reductase (*64*). As such, it is possible that the oxidized nucleotide is required to dissociate from the nNOS to allow the disporportionation of electrons on the flavins to favor the reduction of DCIP, thereby restricting the kinetic mechanism to the exclusive formation of binary enzyme−substrate complexes.

According to the two-site ping-ping mechanism, NADPH oxidation and cytochrome c^{3+} reduction operate independently during nNOS catalytic turnover. This catalytic independence may be facilitated by topographically separate substrate binding sites on nNOS and/or by FMN acting as the terminal electron donator. On the basis of sequence comparisons, the nNOS reductase domain and CPR belong to a class of dual flavin-containing proteins that have independent NADPH/FAD and FMN binding domains (*65*). Mutational analysis and sequence comparison with CPR suggests that cytochrome c^{3+} interacts with a cluster of acidic residues in the FMN domain, while NADPH binds in proximity to FAD (*29*). Therefore, if the substrates bind to different domains, which are separated by an internal electron carrier that stores reducing equivalents, independent reactions with either substrate could occur.

Comparison of the inhibition constants for 2′AMP determined with DCIP or cytochrome c^{3+} as the electron acceptor led to the second modification of the mechanisms proposed for DCIP and cytochrome c^{3+} reduction. In both the iso ping-pong and the (two-site) ping-pong mechanisms, the NADPH analogue binds to the same enzyme form as NADPH, E_1. This is consistent with the 2′AMP dead-end inhibition patterns listed in Tables 2 and 3; however, if 2′AMP bound to E_1 in both mechanisms, then the values of the inhibition constants for 2′AMP should be the same regardless of the electron acceptor. Nevertheless, a large increase in the apparent affinity for 2′AMP in the presence of DCIP compared to that for cytochrome c^{3+} was observed. To interpret these results, an additional free enzyme form, E_1', was proposed to occur in both mechanisms. The differences in the inhibition constants for 2′AMP would arise if the following conditions were met: (1) the NADPH analogue could only form dead-end complexes with E_1' and not E_1,

E_3, or, in the case of cytochrome c^{3+}, E_2; (2) NADPH and $NADP^+$ could not bind to E_1'; and (3) E_1 is in rapid equilibrium with E_1'. The last assumption still results in a competitive inhibition pattern for 2′AMP versus NADPH. The kinetic mechanisms proposed for DCIP and cytochrome c^{3+} were revised to include the isomerization step for the free enzyme governed by the equilibrium constant, K (Figures 3 and 4). The two mechanisms also include different dead-end complexes between E_1' and 2′AMP which could account for the differences in the apparent affinity of 2′AMP observed in dead-end inhibition studies.

On the basis of sequence homology, the putative $NADP^+$ and FAD binding motifs of nNOS belong to the flavoenzyme family of which ferridoxin−$NADP^+$ reductase (FNR) is the prototype. The early crystal structure of FNR failed to reveal the geometry between FAD and the nicotinamide ring. The only relevant structural information was obtained with the 2′AMP portion of the $NADP^+$ molecule complexed with the enzyme (*66*). This occurred because positioning of the nicotinamide ring in proximity to the *re* face of the FAD cofactor required the energetically unfavorable displacement of a tyrosine residue (*67*). The two alternate forms of nNOS, E_1 and E_1', may likewise result from the positioning of a similar residue in nNOS.

Rate equations were derived for the proposed di-iso ping-pong bi-bi mechanism for DCIP and the iso (two-site) ping-pong mechanism for cytochrome c^{3+} under initial velocity conditions and for product and dead-end inhibition studies (Appendix). The derivation of the nNOS-catalyzed reduction of cytochrome c^{3+} is similar to the derivation for the CPR-catalyzed reduction which assumes that the binding and release of ligands occur in rapid equilibrium and the conversion of enzyme forms (i.e., E_1 to E_3) occurs at steady state. This assumption was also used for the derivation of the nNOS-catalyzed reduction of DCIP. All of the experimental initial velocity and inhibition patterns were consistent with the patterns predicted for the rate equations derived under the appropriate conditions. The turnover rate (k_{cat}), the Michaelis constant (K_m), and the values for k_{cat}/K_m for each substrate are also defined in terms of rate and equilibrium constants in the Appendix [i.e., $(k_{cat}/K_m)_{NADPH} = k_3/K_{iA}(1 + 1/K)$ (Figures 3 and 4), $(k_{cat}/K_m)_{DCIP} = k_7k_{11}/K_{iB}(k_7 + k_8)$ (Figure 3), and $(k_{cat}/K_m)_{cytc} = k_9k_{15}/K_{iB}(k_9 + k_{15})$ (Figure 4)]. The ratio of rate and equilibrium constants for defining $(k_{cat}/K_m)_{NADPH}$ was the same for both mechanisms.

Although Ca^{2+}-CaM increased the rate of DCIP and cytochrome c^{3+} reduction, it did not change the proposed kinetic mechanism for the reduction of either electron acceptor. Identical types of initial velocity, product, and dead-end inhibition patterns were observed in the presence or absence of Ca^{2+}-CaM. The presence of the activated cofactor did have variable effects on the kinetic parameters for the various substrates listed in Table 1 and on the inhibition constants listed in Tables 2 and 3. The influence of Ca^{2+}-CaM on these various parameters will be discussed in the context of the mechanisms presented in Figures 3 and 4 in an effort to describe how individual rate constants are affected.

$NADP^+$ is a competitive inhibitor of NADPH in the presence of nonsaturating concentrations of cytochrome c^{3+}; therefore, the reported K_{is} is a direct measure of the dissociation constant for $NADP^+$. The presence of Ca^{2+}-CaM in the inhibition study caused a 2-fold increase in the inhibition constant for $NADP^+$, suggesting that it may slightly reduce the affinity of the enzyme for $NADP^+$. The activated cofactor also caused an increase in the K_{is} of 2′AMP versus NADPH with either DCIP or cytochrome c^{3+} as the electron acceptor. Although the dead-end inhibitor is also competitive versus NADPH, the K_{is} value is not a direct measure of the dissociation constant because it is also a function of the equilibrium constant K, equal to $[E_1]/[E_1']$, (eqs A19, A20, and A39 in the Appendix). If it is assumed that Ca^{2+}-CaM has a negligible effect on the equilibrium between E_1 and E_1', the increase in the K_{is} value for 2′AMP may be interpreted as the ability of the cofactor to slightly reduce the affinity of nNOS for 2′AMP. The activated cofactor also caused a 1.5-fold increase in $(k_{cat}/K_m)_{NADPH}$ with DCIP as an electron acceptor (Table 1). While the average value of $(k_{cat}/K_m)_{NADPH}$ with cytochrome c^{3+} increased ∼2-fold in the presence of Ca^{2+}-CaM, the large error associated with the value, which originates with the difficulty in determining the low K_m for NADPH under these conditions, did not make the change significant (Table 1). If it is assumed that the 1.5−2-fold increase in $(k_{cat}/K_m)_{NADPH}$ is valid for both acceptors, it would be do to an increase in the value of the expression $k_3/K_{iA}(1 + 1/K)$ (Appendix). Thus, the presence of Ca^{2+}-CaM could affect either the rate of hydride transfer, k_3, the dissociation constant for NADPH, K_{iA}, or both.

Ca^{2+}-CaM caused a 4.5-fold increase in $(k_{cat}/K_m)_{DCIP}$ and a 23-fold increase in $(k_{cat}/K_m)_{cytc}$ (Table 1). Both of these kinetic parameters are defined by the ratio of forward rate constants for the reduction of the electron acceptor in the second half-reaction (k_7 and k_{11} for DCIP and k_9 and k_{15} for cytochrome c^{3+}) as well as their associated binding constants shown in eqs 6 and 7. K_{iB} is the dissociation constant for

$$(k_{cat}/K_m)_{DCIP} = \frac{k_7k_{11}}{K_{iB}(k_7 + k_8)} \quad (6)$$

$$(k_{cat}/K_m)_{cytc} = \frac{k_9k_{15}}{K_{iB}(k_9 + k_{15})} \quad (7)$$

DCIP and cytochrome c^{3+} in eqs 6 and 7, respectively. The rate constants k_7, k_8, and k_{11} in eq 6 are the same as those in Figure 3, and the rate constants k_9 and k_{15} in eq 7 are the same as those in Figure 4. The data suggest that the binding of Ca^{2+}-CaM may stimulate the rate of electron transfer to the electron acceptors by increasing the forward rate constants for these steps and/or decreasing the dissociation constant for the electron acceptor.

The presence of Ca^{2+}-CaM also caused an approximate 2-fold increase in the Michaelis constant for NADPH, K_{NADPH}, with DCIP as an electron acceptor and a 10-fold increase with cytochrome c^{3+} as an electron acceptor. Equations 8 and 9 define K_{NADPH} in terms of rate and equilibrium constants according to the derivation of the mechanisms proposed for the reduction of DCIP and cytochrome c^{3+}, respectively.

$$K_{NADPH} = \frac{K_{iA}(1 + 1/K)}{(1 + k_3/k_7 + k_3/k_{11})} \quad (8)$$

The rate constants k_3, k_7, and k_{11} in eq 8 are the same as

$$K_{NADPH} = \frac{K_{iA}(1 + 1/K)}{(1 + k_3/k_9 + k_3/k_{15})} \quad (9)$$

those in Figure 3, and the rate constants k_3, k_9, and k_{15} in eq 7 are the same as those in Figure 4. The reason Ca^{2+}-CaM exerts more of a change in K_{NADPH} with cytochrome c^{3+} may be the difference in the ratios of rate and equilibrium constants defined for K_{NADPH}. If it is assumed that Ca^{2+}-CaM had no effect on K, then the increase in K_{NADPH} may be do to the decrease in k_3/k_9 and/or k_3/k_{15} ratios. In other words, Ca^{2+}-CaM accelerates electron transfer to cytochrome c^{3+} by increasing k_9 and/or k_{15} to a greater extent then its stimulation of hydride transfer given by k_3. The Ca^{2+}-CaM-induced increase in k_9 and/or k_{15} also agrees well with the large increase (23-fold) in $(k_{cat}/K_m)_{cytc}$ (eq 7). Similarly, the 2-fold change in K_{NADPH} with DCIP may be caused by changes in k_3/k_7 and/or k_3/k_{11} ratios.

The presence of Ca^{2+}-CaM does not significantly change the K_{ii} for 2′AMP with either DCIP or cytochrome c^{3+} as the variable substrate. For DCIP, this observation is consistent with the reaction occurring in two half-reactions, and for cytochrome c^{3+}, the observation is also consistent with the two half-reactions occurring at two separate catalytic sites on the enzyme.

In summary, we have shown that the nNOS-catalyzed reduction of DCIP and the nNOS-catalyzed reduction of cytochrome c^{3+} are accommodated by the di-iso ping-pong bi-bi mechanism and by the iso (two-site) ping-pong mechanism, respectively. Although the presence of Ca^{2+}-CaM accelerates the rate of electron transfer, its presence does not alter either of these mechanisms.

ACKNOWLEDGMENT

We are grateful to Drs. Sonia Anderson and Dean Malencik for supplying CaM and the CaM-Sepharose column and to Dr. Ted Dawson for giving us the cDNA plasmid construct for rat neuronal NOS. We also acknowledge the Nucleic Acids and Proteins Core Facilities of the Oregon State University Environmental Health Sciences Center in conducting these studies.

APPENDIX

Derivation of the Rate Equation for a Di-Iso Ping-Pong Bi-Bi Mechanism for nNOS-Catalyzed Reduction of DCIP. Figure 3 shows the kinetic scheme for the di-iso ping-pong mechanism proposed for the nNOS-catalyzed reduction of DCIP. The basic features of the proposed mechanism are as follows. (a) The reaction consists of two half-reactions with NADPH oxidation reducing the enzyme to the three-electron-reduced state, E_3, followed by reduction of DCIP which converts the enzyme back to the one-electron-reduced state, E_1. (b) A steady-state isomerization step occurs between two forms of the three-electron-reduced state of the enzyme, E_3 and E_3', one that binds $NADP^+$ and one that binds DCIP. (c) An alternate form of the free enzyme, E_1', exists in the reaction sequence, which is in rapid equilibrium with E_1 and is able to bind the NADPH analogue, 2′AMP, but not the substrate NADPH. The binding of substrates and/or inhibitors and the release of products are assumed to occur in rapid equilibrium; thus, the kinetic mechanism is divided into three rapid equilibrium segments, labeled X, Y, and Z. The steady-state equation was derived according to the method of Cha (*68*). For the purposes of illustrating how dead-end inhibition studies with 2′AMP lead to the proposal of the rapid isomerization of E_1 to E_1' in the overall reaction scheme, the enzyme−inhibitor complexes that would form with the substrate analogue, 2′AMP (I), are also included in Figure 3. The fractionation factors for the mechanism drawn in Figure 3 are as follows:

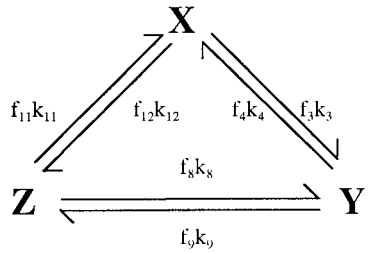

FIGURE 5: Steady-state steps for the nNOS-catalyzed reduction of DCIP. X, Y, and Z refer to the rapid equilibrium segments drawn in Figure 3. *X* represents all the enzyme species that bind NADPH, 2′AMP, and $DCIP_{red}$; *Y* represents all the enzyme species that bind $NADP^+$, and *Z* represents all the enzyme species that bind $DCIP_{ox}$ (i.e., $X = E_1 + E_1' + E_1'I + E_1'IQ + E_1'Q + E_1A$; $Y = E_3P + E_3$; $Z = E_3' + E_3'B$). The f_i represents the fractional concentration of rapid equilibrium segment involved in the reaction given by the rate constants k_i (eqs A1−A6).

$$f_3 = \frac{E_1A}{X} = (A/K_{iA})/[1 + A/K_{iA} + (1/K)(1 + I/K_{iI} + Q/K_{iQ} + QI/K_{iQ}K_{iI})] \quad (A1)$$

$$f_4 = \frac{E_3P}{Y} = \frac{P/K_{iP}}{1 + P/K_{ip}} \quad (A2)$$

$$f_7 = \frac{E_3}{Y} = \frac{1}{1 + P/K_{ip}} \quad (A3)$$

$$f_8 = \frac{E_3'}{Z} = \frac{1}{1 + B/K_{iB}} \quad (A4)$$

$$f_{11} = \frac{E_3'B}{Z} = \frac{B/K_{iB}}{1 + B/K_{iB}} \quad (A5)$$

$$f_{12} = \frac{E_1'Q}{X} = (Q/K_{iQ})/[1 + A/K_{iA} + (1/K)(1 + I/K_{iI} + Q/K_{iQ} + QI/K_{iQ}K_{iI})] \quad (A6)$$

where *A*, *B*, *P*, *Q*, and *I* represent NADPH, $DCIP_{ox}$, $NADP^+$, $DCIP_{red}$, and 2′AMP concentrations, respectively, and the K_i values refer to their respective dissociation constants. E_1 and E_1' are the one-electron (FAD-$FMNH^\bullet$) forms of nNOS that exclusively bind NADPH and 2′AMP, respectively. E_3 and E_3' are the three-electron ($FADH^\bullet$-$FMNH_2$) or ($FADH_2$-$FMNH^\bullet$) forms of nNOS that exclusively bind $NADP^+$ and $DCIP_{ox}$, respectively. *K* (equal to E_1/E_1') is the equilibrium constant for the conversion of the two free enzyme forms, E_1 and E_1'. $X = E_1 + E_1' + E_1'I + E_1'IQ + E_1'Q + E_1A$. $Y = E_3P + E_3$. $Z = E_3' + E_3'B$. $E_t = X + Y + Z$. Using the scheme shown in Figure 5 as the basic King−Altman figure, the following velocity equation is obtained:

$$\frac{v_i}{E_t} = (k_3k_7k_{11}f_3f_7f_{11} - k_4k_8k_{12}f_4f_8f_{12})/(k_4k_8f_4f_8 + k_4k_{11}f_4f_{11} + k_7k_{11}f_7f_{11} + k_3k_8f_3f_8 + k_3k_{11}f_3f_{11} + k_8k_{12}f_8f_{12} + k_3k_7f_3f_7 + k_4k_{12}f_4f_{12} + k_7k_{12}f_7f_{12}) \quad (A7)$$

Under initial velocity conditions ($P = Q = I = 0$), substitution of the fractionation factors (eqs A1−A6) into eq A7 yields the following equation:

$$\frac{v_i}{E_t} = \{[A][B][k_3k_7k_{11}/(k_3k_7 + k_3k_{11} + k_7k_{11})]\}/\{[A][B] + [B][K_{iA}(1 + 1/K)k_7k_{11}/(k_3k_7 + k_3k_{11} + k_7k_{11})] + [A][K_{iB}(k_3k_7 + k_3k_8)/(k_3k_7 + k_3k_{11} + k_7k_{11})]\} \quad (A8)$$

The kinetic constants are defined as follows:

$$k_{cat} = \frac{k_3k_7k_{11}}{k_3k_7 + k_3k_{11} + k_7k_{11}} \quad (A9)$$

$$K_A = \frac{K_{iA}k_7k_{11}(1 + 1/K)}{k_3k_7 + k_3k_{11} + k_7k_{11}} \quad (A10)$$

$$K_B = \frac{K_{iB}(k_3k_7 + k_3k_8)}{k_3k_7 + k_3k_{11} + k_7k_{11}} \quad (A11)$$

Equation A8 simplifies to eq A12.

$$\frac{v_i}{E_t} = \frac{V[A][B]}{[A][B] + K_B[A] + K_A[B]} \quad (A12)$$

which has the same form as the rate equation for a ping-pong mechanism, eq 1. Thus, the proposed mechanism for nNOS reduction of DCIP is consistent with the observed initial velocity patterns and yields the same patterns expected for a standard ping-pong mechanism.

(1) Product Inhibition. The equation describing product inhibition by $NADP^+$, P, is derived letting $Q = I = 0$ and substituting the fractionation factors from eqs A1−A6 into eq A7:

$$\frac{v_i}{E_t} = (V[A][B])/[[A][B] + K_B[A] + K_A[B] + [P](D_1/K_{iP}) + [A][P](D_2/K_{iP}) + [B][P](D_3/K_{iP}) + [A][B][P](D_4/K_{iP})] \quad (A13)$$

where

$$D_1 = \frac{K_{iB}K_{iA}k_4k_8(1 + 1/K)}{k_7k_{11} + k_3k_{11} + k_3k_7} \quad (A14)$$

$$D_2 = \frac{K_{iB}(k_3k_8 + k_4k_8)}{k_7k_{11} + k_3k_{11} + k_3k_7} \quad (A15)$$

$$D_3 = \frac{K_{iA}k_4k_{11}(1 + 1/K)}{k_7k_{11} + k_3k_{11} + k_3k_7} \quad (A16)$$

$$D_4 = \frac{k_3k_{11} + k_4k_{11}}{k_7k_{11} + k_3k_{11} + k_3k_7} \quad (A17)$$

The double-reciprocal form of eq A13 predicts noncompetitive inhibition patterns for P with either A or B as the variable substrate. Thus, the mechanism correctly predicts the product inhibition patterns which where obtained experimentally.

(2) Dead-End Inhibition. For dead-end inhibition by the substrate analogue, 2′AMP (I), $P = Q = 0$, substitution of eqs A1−A6 into eq A7 yields the following velocity equation:

$$\frac{v_i}{E_t} = (V[A][B])/([A][B] + K_B[A] + K_A[B]\{1 + [I]/[K_{il}(1 + K)]\}) \quad (A18)$$

With A as the varied substrate, the double-reciprocal form of eq A18 is

$$\frac{E_t}{v_i} = \frac{1}{V}\left(1 + \frac{K_B}{B}\right) + \frac{K_A}{V}\left[1 + \frac{[I]}{K_{il}(1 + K)}\right]\frac{1}{[A]} \quad (A19)$$

The equation predicts a competitive pattern for I when A is the variable substrate, consistent with the experimental results. When eq A19 is arranged with B as the variable substrate, the equation becomes

$$\frac{E_t}{v_i} = \frac{1}{V}\left\{1 + \frac{K_A}{A}\left[1 + \frac{[I]}{K_{il}(1 + K)}\right]\right\} + \frac{K_B}{V}\frac{1}{[B]} \quad (A20)$$

Uncompetitive inhibition is predicted for I when B is the variable substrate, consistent with the experimental results. Comparison of eq 2 with eq A19 and eq 3 with eq A20 shows that the K_{is} and K_{ii} values are both a function of the dissociation constant, K_{il}, and the equilibrium constant, K, between E_1 and E_1'.

Derivation of Rate Equations of an Iso Two-Site Ping-Pong Mechanism for nNOS-Catalyzed Reduction of Cytochrome c^{3+}. Figure 4 shows the kinetic scheme for the iso two-site ping-pong mechanism with NADPH binding in a uni-uni fashion at site 1 and cytochrome c^{3+} binding in a tert-uni ping-pong fashion at site 2. Although the reaction consists of two half-reactions, the two active sites operate independently and formation of a ternary complex is possible. Since the difference in the apparent affinity for 2′AMP obtained with DCIP compared to that with cytochrome c^{3+} as an electron acceptor led to the proposal that the reaction proceeds via an iso mechanism, Figure 4 also shows 2′AMP forming a dead-end complex with E_1'. To simplify the derivation of the rate equation, the following assumptions were made: (1) all ligand binding steps occur in rapid equilibrium, (2) the binding of a ligand at site 1 does not effect of binding of the ligands at site 2, and (3) the values of all ligand dissociation constants are unaffected by the oxidation state of the enzyme. Figure 6A illustrates the number of different binary and ternary complexes that can form with nNOS and the various ligands, and Figure 6B

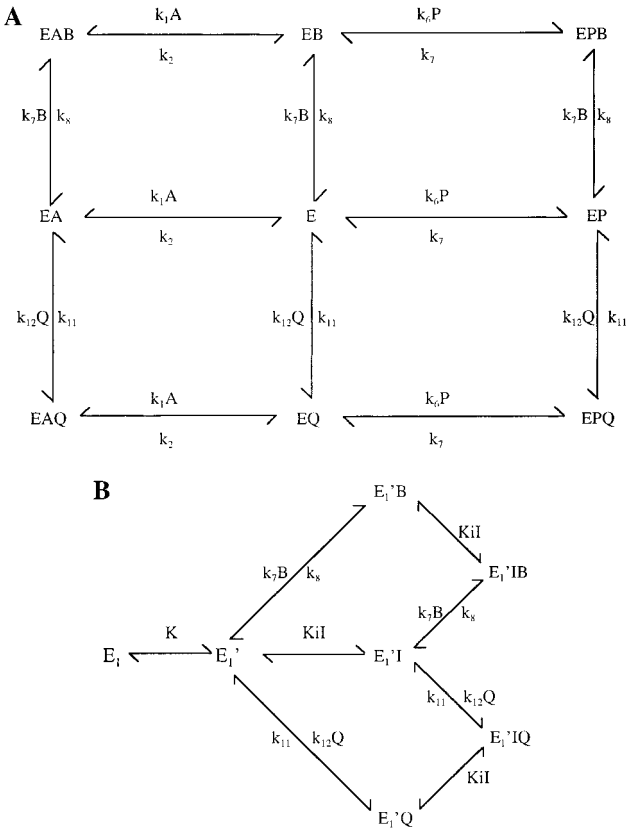

FIGURE 6: Kinetic scheme showing the various rapid equilibrium enzyme−ligand complexes that form in the iso (two-site) ping-pong mechanism for the nNOS-catalyzed reduction of cytochrome c^{3+}. A, B, P, Q, and I represent the same molecules as in Figure 4, and the rate and equilibrium constants are the same as those in Figure 4. In panel A, E represents E_1, E_2, or E_3. Panel B illustrates the equilibrium between E_1, the free enzyme form that binds NADPH but not 2′AMP, and E_1', the free enzyme form that binds 2′AMP but not NADPH.

shows the additional dead-end complexes that form with E_1' in the presence of 2′AMP. Equations were derived using the method of Cha (*62*) with the fractionation factors defined as follows:

$$f_A = (E_1A + E_1AB + E_1AQ)/E_{tX} = (A/K_{iA})/[1 + A/K_{iA} + P/K_{iP} + 1/K(1 + I/K_{iI})] \quad \text{(A21)}$$

$$f_B = (E_2B + E_2AB + E_2PB)/E_{t2} = (E_3B + E_3AB + E_3PB)/E_{t3} = (B/K_{iB})/(1 + B/K_{iB} + Q/K_{iQ}) \quad \text{(A22)}$$

$$f_P = (E_3P + E_3PB + E_3PQ)/E_{t3} = (P/K_{iP})/(1 + A/K_{iA} + P/K_{iP}) \quad \text{(A23)}$$

$$f_Q = (E_2Q + E_2AQ + E_2PQ)/E_{t2} = (Q/K_{iQ})/(1 + B/K_{iB} + Q/K_{iQ}) \quad \text{(A24)}$$

$$f_Q' = (E_1'Q)/E_{tX} = (Q/KK_{iQ})/\{(1 + B/K_{iB} + Q/K_{iQ})[1 + A/K_{iA} + P/K_{iP} + 1/K(1 + I/K_{iI})]\} \quad \text{(A25)}$$

where *A*, *B*, *P*, *Q*, and *I* represent NADPH, cytochrome c^{3+}, $NADP^+$, cytochrome c^{2+}, and 2′AMP concentrations, respectively, and the K_i values refer to the respective dissociation constants. E_1 and E_1' are the one-electron (FAD-$FMNH^\bullet$)

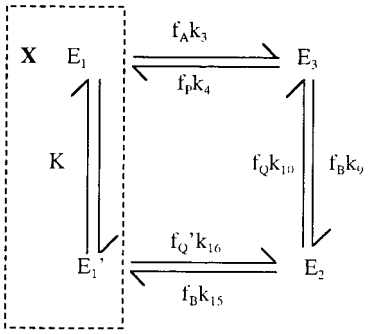

FIGURE 7: Steady-state steps for the nNOS-catalyzed reduction of cytochrome c^{3+}. E_1, E_1', E_2, and E_3, the rate constants, and *K* are the same as in Figure 4. The dotted box labeled X represents the rapid equilibrium segments between E_1 and E_1', and the values for the fractionation factors, f_i, are given in eqs A21−A25.

forms of nNOS that exclusively bind NADPH and 2′AMP, respectively. E_2 is the two-electron (FAD-$FMNH_2$) enzyme form, and E_3 is the three-electron ($FADH^\bullet$-$FMNH_2$) form of the enzyme. *K* (equal to E_1/E_1') is the equilibrium constant for the conversion of the two free enzyme forms. $E_{t2} = E_2 + E_2A + E_2B + E_2P + E_2Q + E_2AB + E_2BP + E_2AQ + E_2PQ$. $E_{t3} = E_3 + E_3A + E_3B + E_3P + E_3Q + E_3AB + E_3BP + E_3AQ + E_3PQ$. $E_{tX} = E_1 + E_1A + E_1B + E_1P + E_1Q + E_1AB + E_1BP + E_1AQ + E_1PQ + E_1' + E_1'I + E_1'B + E_1'Q + E_1'IB + E_1'IQ$. Using the fractionation factors and the scheme in Figure 7 as the basic King−Altman pattern, one can derive the following velocity equation:

$$\frac{v_i}{E_t} = (k_3k_9k_{15}f_Af_Bf_B - k_4k_{10}k_{16}f_Pf_Qf_Q')/(k_4k_{10}f_Pf_Q + k_4k_{15}f_Pf_B + k_9k_{15}f_Bf_B + k_3k_9f_Af_B + k_4k_6f_Pf_Q' + k_9k_{16}f_Bf_Q' + k_3k_{10}f_Af_Q + k_3k_{15}f_Af_B + k_{10}k_{16}f_Qf_Q') \quad \text{(A26)}$$

Under initial velocity conditions ($P = Q = I = 0$), substitution of the fractionation factors defined in eqs A21−A25 simplifies the overall rate equation to the following equation.

$$\frac{v_i}{E_t} = [(k_3k_9k_{15}[A][B])/(k_3k_9 + k_3k_{15} + k_9k_{15})]/([A][B] + [A]\{[K_{iB}(k_3k_{15} + k_3k_9)]/(k_3k_9 + k_3k_{15} + k_9k_{15})\} + [B]\{[K_{iA}k_9k_{15}(1 + 1/K)]/(k_3k_9 + k_3k_{15} + k_9k_{15})\}) \quad \text{(A27)}$$

Kinetic constants are defined in eqs A28−A30.

$$k_{cat} = \frac{k_3k_9k_{15}}{k_3k_9 + k_3k_{15} + k_9k_{15}} \quad \text{(A28)}$$

$$K_A = \frac{K_{iA}k_9k_{15}(1 + 1/K)}{k_3k_9 + k_3k_{15} + k_9k_{15}} \quad \text{(A29)}$$

$$K_B = \frac{K_{iB}(k_3k_{15} + k_3k_9)}{k_3k_9 + k_3k_{15} + k_9k_{15}} \quad \text{(A30)}$$

Thus, the rate equation reduces to the following:

$$\frac{v_i}{E_t} = \frac{V[A][B]}{[A][B] + K_B[A] + K_A[B]} \quad \text{(A31)}$$

K_A and K_B refer to the Michaelis constants of NADPH and

cytochrome c^{3+}, respectively, and V is the maximal velocity. Equation A31 has the same form as eq 1, to which the parallel initial velocity patterns were fit. Thus, the proposed two-site ping-pong mechanism for nNOS reduction of cytochrome c^{3+} is consistent with the observed initial velocity patterns. However, a hexa-uni one-site ping-pong mechanism would also generate a rate equation having the same form as the equation for the two-site ping-pong mechanism under initial velocity conditions. Therefore, product and dead-end inhibition studies were required to distinguish which mechanism is valid for nNOS.

(1) Product Inhibition Patterns. In the CPR-catalyzed reduction of cytochrome c^{3+}, $NADP^+$ is uncompetitive versus cytochrome c^{3+}. Sem and Kasper accounted for this inhibition pattern by assuming that electron transfer from E_3 to cytochrome c^{3+} is much faster than electron transfer from E_3 to $NADP^+$ (i.e., $k_9 \gg k_4$) (*50*). This assumption was supported by the absence of pronounced curvature in the double-reciprocal plots with cytochrome c^{2+} as an inhibitor. Since $NADP^+$ is uncompetitive versus cytochrome c^{3+} and the double-reciprocal plots with cytochrome c^{2+} as an inhibitor are linear, the same assumptions were made for the nNOS mechanism. In the presence of P ($Q = I = 0$), substitution of the fractionation factors defined in eqs A21−A25 into eq A26 and omission of terms in eq A26 containing k_4 gave the following equation:

$$\frac{v_i}{E_t} = (V[A][B])/([A][B] + [B]K_A + [A]K_B + [B][P]\{K_A/[K_{iP}(1 + 1/K)]\}) \quad \text{(A32)}$$

Equation A32 predicts competitive inhibition by P when A is the variable substrate. The corresponding equation describing product inhibition by P with B as the variable substrate predicts uncompetitive inhibition. Thus, the mechanism correctly predicts the product inhibition patterns obtained experimentally.

With product inhibition by Q ($P = I = 0$), substitution of the fractionation factors defined in eqs A21−A25 into eq A26 produces the following rate equation:

$$\frac{v_i}{E_t} = (V[A][B]^2)/([A][B]^2 + [B]^2K_A + [A][B]K_B + [A][B][Q](C_1/K_{iQ}) + [B][Q](C_2/KK_{iQ}) + [A][Q](C_3/K_{iQ}) + [A][Q]^2(C_3/K_{iQ}^2) + [Q]^2(C_4/KK_{iQ}^2)] \quad \text{(A33)}$$

where

$$C_1 = K_{iB}[(k_3k_9 + k_3k_{10} + k_3k_{15})/(k_3k_9 + k_9k_{15} + k_3k_{15})] \quad \text{(A34)}$$

$$C_2 = K_{iA}K_{iB}[k_9k_{16}/(k_3k_9 + k_9k_{15} + k_3k_{15})] \quad \text{(A35)}$$

$$C_3 = K_{iB}^2[k_3k_{10}/(k_3k_9 + k_9k_{15} + k_3k_{15})] \quad \text{(A36)}$$

$$C_4 = K_{iA}K_{iB}^2[k_{10}k_{16}/(k_3k_9 + k_9k_{15} + k_3k_{15})] \quad \text{(A37)}$$

The terms C_1 and C_2 predominate over C_3 and C_4 in eq A33 since k_{10} and k_{16}, which represent the rate of cytochrome c^{2+} reduction of E_2 and E_1, respectively, are assumed to be much slower than electron transfer to cytochrome c^{3+}, k_9 and k_{15}. This assumption is based on the absence of curvature in the initial velocity patterns. Furthermore, if hydride transfer, k_3, is much slower than electron transfer to cytochrome c^{3+}, then $C_2 \gg C_3$. Both of these assumptions were also made in the derivation of the rate equation for cytochrome c^{2+} inhibition studies with CPR (*50*). Thus, eq A33 reduces to the following equation:

Scheme 5

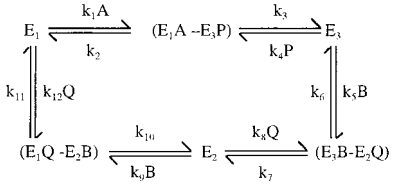

$$\frac{v_i}{E_t} = (V[A][B])/([A][B] + [B]K_A + [A]K_B + [A][Q](C_1/K_{iQ}) + [Q](C_2/KK_{iQ})] \quad \text{(A38)}$$

Equation A38 predicts product inhibition by Q with B as the variable substrate to be competitive. The corresponding equation describing product inhibition by Q with A as the variable substrate predicts noncompetitive inhibition. Therefore, the proposed iso two-site ping-pong mechanism is consistent with the cytochrome c^{2+} product inhibition patterns obtained experimentally.

(2) Dead-End Inhibition by 2′AMP. In the presence of 2′AMP, I ($P = Q = 0$), substitution of the fractionation factors defined in eqs A21−A25 into eq A26 leads to the following equation:

$$\frac{v_i}{E_t} = (V[A][B])/([A][B] + K_B[A] + K_A[B]\{1 + [I]/[K_{iI}(1 + K)]\}) \quad \text{(A39)}$$

Equation A39 predicts that I will be competitive versus A and uncompetitive versus B. As with the di-iso ping-pong mechanism described for DCIP as an electron acceptor, the overall apparent affinity for 2′AMP is a function of its dissociation constant and the equilibrium constant, K (equal to E_1/E_1'); i.e., $K_{is} = K_{iI}(1 + K)$, and $K_{ii} = K_{iI}(1 + K)$.

Derivation of the Rate Equation Describing a Hexa-Uni Ping-Pong Mechanism for nNOS-Catalyzed Reduction of Cytochrome c^{3+}. Scheme 5 shows the kinetic scheme for the hexa-uni ping-pong mechanism with NADPH binding in a uni-uni fashion followed by the binding of cytochrome c^{3+} in a tert-uni ping-pong fashion. The reaction consists of two half-reactions with only the formation of binary complexes possible. Using Scheme 5 as the basic King−Altman figure, the following rate equation is obtained.

$$\frac{v_i}{E_t} = (k_1k_3k_5k_7k_9k_{11}[A][B]^2 - k_2k_4k_6k_8k_{10}k_{12}[P][Q]^2)/[[A][B]^2(k_1k_5k_7k_9k_{11} + k_1k_3k_5k_9k_{11} + k_1k_3k_5k_7k_9) + [B]^2(k_3k_5k_7k_9k_{11} + k_2k_5k_7k_9k_{11}) + [A][B](k_1k_3k_7k_9k_{11} + k_1k_3k_6k_9k_{11} + k_1k_3k_5k_7k_{11} + k_1k_3k_5k_7k_{10}) + [B][P](k_2k_4k_6k_9k_{11} + k_2k_4k_7k_9k_{11}) + [A][B][P](k_1k_4k_6k_9k_{11} + k_1k_4k_7k_9k_{11}) + [Q]^2(k_3k_6k_8k_{10}k_{12} + k_2k_6k_8k_{10}k_{12}) + [A][Q](k_1k_3k_6k_8k_{11} + k_1k_3k_6k_8k_{10}) + [B][Q]^2(k_3k_5k_8k_{10}k_{12} + k_2k_5k_8k_{10}k_{12}) + [A][B][Q](k_1k_3k_5k_8k_{11} + k_1k_3k_5k_8k_{10}) + [B][Q](k_3k_5k_7k_{10}k_{12} + k_2k_5k_7k_{10}k_{12}) + [B]^2[Q](k_3k_5k_7k_9k_{12} + k_2k_5k_7k_9k_{12}) + [P][Q](k_2k_4k_7k_{10}k_{12} + k_2k_4k_6k_{10}k_{12} + k_2k_4k_6k_8k_{11} + k_2k_4k_6k_8k_{10}) + [P][Q]^2(k_2k_4k_8k_{10}k_{12} + k_2k_4k_6k_8k_{12} + k_2k_4k_8k_{10}k_{12}) + [A][P][Q](k_1k_4k_6k_8k_{11} + k_1k_4k_6k_8k_{10}) + [B][P][Q](k_2k_4k_7k_9k_{12} + k_2k_4k_6k_9k_{12})] \quad (A40)$$

Equation A40 simplifies to the following equation under initial velocity conditions ($P = Q = 0$).

$$\frac{v_i}{E_t} = (k_1k_3k_5k_7k_9k_{11}[A][B])/[[A][B](k_1k_5k_7k_9k_{11} + k_1k_3k_5k_9k_{11} + k_1k_3k_5k_7k_9) + [B](k_3k_5k_7k_9k_{11} + k_2k_5k_7k_9k_{11}) + [A](k_1k_3k_7k_9k_{11} + k_1k_3k_6k_9k_{11} + k_1k_3k_5k_7k_{11} + k_1k_3k_5k_7k_{10})] \quad (A41)$$

The kinetic constants are defined in eqs A42−A44.

$$k_{cat} = (k_3k_7k_{11})/(k_7k_{11} + k_3k_{11} + k_3k_7) \quad (A42)$$

$$K_A = [k_7k_{11}(k_2 + k_3)]/[k_1(k_7k_{11} + k_3k_{11} + k_3k_7)] \quad (A43)$$

$$K_B = [k_3(k_7k_9k_{11} + k_6k_9k_{11} + k_5k_7k_{11} + k_5k_7k_{10})]/[k_5k_9(k_7k_{11} + k_3k_{11} + k_3k_7)] \quad (A44)$$

where K_A and K_B refer to the Michaelis constants of NADPH and cytochrome c^{3+}, respectively. Equation A41 reduces to the following equation:

$$\frac{v_i}{E_t} = \frac{V[A][B]}{[A][B] + K_B[A] + K_A[B]} \quad (A45)$$

which has the same form as eq 1 to which the parallel initial velocity patterns were fit. Thus, the proposed hexa-uni ping-pong mechanism for nNOS reduction of cytochrome c^{3+} is consistent with the observed initial velocity patterns.

(1) Product Inhibition Patterns. With product inhibition by P ($Q = 0$), eq A40 reduces to the following equation:

$$\frac{v_i}{E_t} = (k_1k_3k_5k_7k_9k_{11}[A][B])/[[A][B](k_1k_5k_7k_9k_{11} + k_1k_3k_5k_9k_{11} + k_1k_3k_5k_7k_9) + [B](k_3k_5k_7k_9k_{11} + k_2k_5k_7k_9k_{11}) + [A](k_1k_3k_7k_9k_{11} + k_1k_3k_6k_9k_{11} + k_1k_3k_5k_7k_{11} + k_1k_3k_5k_7k_{10}) + [P](k_2k_4k_6k_9k_{11} + k_2k_4k_7k_9k_{11}) + [A][P](k_1k_4k_6k_9k_{11} + k_1k_4k_7k_9k_{11})] \quad (A46)$$

Equation A46 can be rewritten as

$$\frac{v_i}{E_t} = (V[A][B])/([A][B] + [A]K_B + [B]K_A + [P]/G_1 + [A][P]/G_2) \quad (A47)$$

where K_A, K_B, and k_{cat} are defined as above and

$$G_1 = \frac{k_1k_5k_9(k_7k_{11} + k_3k_{11} + k_3k_7)}{k_2k_4k_6k_{11}(k_6 + k_7)} \quad (A48)$$

$$G_2 = \frac{k_5(k_7k_{11} + k_3k_{11} + k_3k_7)}{k_4k_{11}(k_6 + k_7)} \quad (A49)$$

In double-reciprocal form, eq A47 becomes

$$\frac{E_t}{v_i} = \frac{K_A}{V}\left(1 + \frac{[P]}{[B]K_AG_1}\right)\frac{1}{[A]} + \frac{1}{V}\left[1 + \frac{K_B}{[B]}\left(1 + \frac{[P]}{K_BG_2}\right)\right] \quad (A50)$$

which shows that P will be noncompetitive with A as the variable substrate. This inhibition pattern is inconsistent with the competitive inhibition pattern observed for $NADP^+$ (P) versus NADPH (A) with cytochrome c^{3+} as the electron acceptor. Arranging eq A50 with B as the variable substrate gives

$$\frac{E_t}{v_i} = \frac{K_B}{V}\left(1 + \frac{[P]}{[A]K_BG_1} + \frac{[P]}{K_BG_2}\right)\frac{1}{[B]} + \frac{1}{V}\left(1 + \frac{K_A}{[A]}\right) \quad (A51)$$

Equation A51 predicts that P will be competitive versus B. This inhibition pattern is also inconsistent with the uncompetitive inhibition pattern observed for $NADP^+$ (P) versus cytochrome c^{3+} (B) in Table 3. Therefore, the hexa-uni ping-pong mechanism is not consistent with the basal and CaM-stimulated reduction of cytochrome c^{3+}.

With Q as a product inhibitor ($P = 0$), eq A40 becomes

$$\frac{E_t}{v_i} = (k_1k_3k_5k_7k_9k_{11}[A][B]^2)/[[A][B]^2(k_1k_5k_7k_9k_{11} + k_1k_3k_5k_9k_{11} + k_1k_3k_5k_7k_9) + [B]^2(k_3k_5k_7k_9k_{11} + k_2k_5k_7k_9k_{11}) + [A][B](k_1k_3k_7k_9k_{11} + k_1k_3k_6k_9k_{11} + k_1k_3k_5k_7k_{11} + k_1k_3k_5k_7k_{10}) + [Q]^2(k_3k_6k_8k_{10}k_{12} + k_2k_6k_8k_{10}k_{12}) + [A][Q](k_1k_3k_6k_8k_{11} + k_1k_3k_6k_8k_{10}) + [B][Q]^2(k_3k_5k_8k_{10}k_{12} + k_2k_5k_8k_{10}k_{12}) + [A][B][Q](k_1k_3k_5k_8k_{11} + k_1k_3k_5k_8k_{10}) + [B][Q](k_3k_5k_7k_{10}k_{12} + k_2k_5k_7k_{10}k_{12}) + [B]^2[Q](k_3k_5k_7k_9k_{12} + k_2k_5k_7k_9k_{12})] \quad (A52)$$

Equation A52 reduces to the following equation

$$\frac{E_t}{v_i} = (V[A][B]^2)/([A][B]^2 + K_B[A][B] + K_A[B]^2 + [Q]^2/J_1 + [A][Q]/J_2 + [B][Q]^2/J_3 + [A][B][Q]/J_4 + [B][Q]/J_5 + [B]^2[Q]/J_6) \quad (A53)$$

where K_A, K_B, and k_{cat} are defined in eqs A42−A44.

$$J_1 = \frac{k_1k_5k_9(k_7k_{11} + k_3k_{11} + k_3k_7)}{k_6k_8k_{10}k_{12}(k_2 + k_3)} \quad \text{(A54)}$$

$$J_2 = \frac{k_5k_9(k_7k_{11} + k_3k_{11} + k_3k_7)}{k_3k_6k_8(k_{10} + k_{11})} \quad \text{(A55)}$$

$$J_3 = \frac{k_1k_9(k_7k_{11} + k_3k_{11} + k_3k_7)}{k_8k_{10}k_{12}(k_2 + k_3)} \quad \text{(A56)}$$

$$J_4 = \frac{k_9(k_7k_{11} + k_3k_{11} + k_3k_7)}{k_3k_8(k_{10} + k_{11})} \quad \text{(A57)}$$

$$J_5 = \frac{k_1k_9(k_7k_{11} + k_3k_{11} + k_3k_7)}{k_7k_{10}k_{12}(k_2 + k_3)} \quad \text{(A58)}$$

$$J_6 = \frac{k_1k_9(k_7k_{11} + k_3k_{11} + k_3k_7)}{k_7k_{12}(k_2 + k_3)} \quad \text{(A59)}$$

In double-reciprocal form with A as the variable substrate, eq A53 becomes.

$$\frac{E_t}{v_i} = \frac{1}{V}\left(K_A + \frac{[Q]^2}{J_1[B]^2} + \frac{[Q]^2}{J_5[B]^2} + \frac{[Q]}{J_6} + \frac{[Q]^2}{J_3[B]}\right)\frac{1}{[A]} + \frac{1}{V}\left(1 + \frac{K_B}{[B]} + \frac{[Q]}{J_2[B]^2} + \frac{[Q]}{J_4[B]}\right) \quad \text{(A60)}$$

Inhibition by Q would generate a double-reciprocal plot in which both the intercept and slope are affected and are nonlinear functions of *Q* and/or *B*. Although Table 3 shows that cytochrome c^{2+}, Q, is noncompetitive versus NADPH, A, the inhibition patterns did not exhibit any curvature; therefore, they are not consistent the hexa-uni ping-pong mechanism. Rearranging eq A60 to show B as the variable substrate gives

$$\frac{E_t}{v_i} = \frac{1}{V}\left[\left(K_B + \frac{[Q]^2}{J_3[A]} + \frac{[Q]}{J_4} + \frac{[Q]}{J_5[A]}\right)\frac{1}{[B]} + \left(\frac{[Q]^2}{J_1[A]}\right)\frac{1}{[B]^2}\right] + \frac{1}{V}\left(1 + \frac{K_A}{[A]} + \frac{[Q]}{J_6[A]}\right) \quad \text{(A61)}$$

When B is the variable substrate, inhibition by Q is expected to have an effect on the intercept and the slope, with the slope a nonlinear function of *Q*. As shown in Table 3, cytochrome c^{2+}, Q, is competitive versus cytochrome c^{3+}, B; therefore, the product inhibition pattern is not consistent with the hexa-uni ping-pong mechanism.

REFERENCES

1. Moncada, S., and Higgs, E. A. (1991) *Eur. J. Clin. Invest. 21*, 361−374.
2. Garthwaite, J., and Boulton, C. L. (1995) *Annu. Rev. Physiol. 57*, 683−706.
3. Marletta, M. A., Tayeh, M. A., and Hevel, J. M. (1990) *Biofactors 2*, 219−225.
4. Nathan, C. F. (1991) *Curr. Opin. Immunol. 3*, 65−70.
5. Stuehr, D. J., and Griffith, O. W. (1992) *Adv. Enzymol. Relat. Areas Mol. Biol. 65*, 287−346.
6. Knowles, R. G., and Moncada, S. (1994) *Biochem. J. 298*, 249−258.
7. Marletta, M. A. (1994) *Cell 78*, 927−930.
8. Schmidt, H. H., Pollock, J. S., Nakane, M., Gorsky, L. D., Forstermann, U., and Murad, F. (1991) *Proc. Natl. Acad. Sci. U.S.A. 88*, 365−369.
9. Cho, H. J., Xie, Q. W., Calaycay, J., Mumford, R. A., Swiderek, K. M., Lee, T. D., and Nathan, C. (1992) *J. Exp. Med. 176*, 599−604.
10. Sheta, E. A., McMillan, K., and Masters, B. S. (1994) *J. Biol. Chem. 269*, 15147−15153.
11. Bredt, D. S., and Snyder, S. H. (1990) *Proc. Natl. Acad. Sci. U.S.A. 87*, 682−685.
12. Hevel, J. M., White, K. A., and Marletta, M. A. (1991) *J. Biol. Chem. 266*, 22789−22791.
13. Bredt, D. S., Hwang, P. M., Glatt, C. E., Lowenstein, C., Reed, R. R., and Snyder, S. H. (1991) *Nature 351*, 714−718.
14. Nishimura, J. S., Martasek, P., McMillan, K., Salerno, J., Liu, Q., Gross, S. S., and Masters, B. S. (1995) *Biochem. Biophys. Res. Commun. 210*, 288−294.
15. White, K. A., and Marletta, M. A. (1992) *Biochemistry 31*, 6627−6631.
16. McMillan, K., Bredt, D. S., Hirsch, D. J., Snyder, S. H., Clark, J. E., and Masters, B. S. (1992) *Proc. Natl. Acad. Sci. U.S.A. 89*, 11141−11145.
17. Crane, B. R., Arvai, A. S., Gachhui, R., Wu, C., Ghosh, D. K., Getzoff, E. D., Stuehr, D. J., and Tainer, J. A. (1997) *Science 278*, 425−431.
18. Abu-Soud, H. M., Yoho, L. L., and Stuehr, D. J. (1994) *J. Biol. Chem. 269*, 32047−32050.
19. Abu-Soud, H. M., and Stuehr, D. J. (1993) *Proc. Natl. Acad. Sci. U.S.A. 90*, 10769−10772.
20. Vermilion, J. L., and Coon, M. L. (1978) *J. Biol. Chem. 253*, 8812−8819.
21. Galli, C., MacArthur, R., Abu-Soud, H. M., Clark, P., Steuhr, D. J., and Brudvig, G. W. (1996) *Biochemistry 35*, 2804−2810.
22. Oprian, D. D., Vatsis, K. P., and Coon, M. J. (1979) *J. Biol. Chem. 254*, 8895−8902.
23. Witteveen, C. F. B., Giovanelli, J., Yim, M. B., Gachhui, R., Stuehr, D. J., and Kaufman, S. (1998) *Biochem. Biophys. Res. Commun. 250*, 36−42.
24. Iyanagi, T., and Mason, F. (1973) *Biochemistry 12*, 2297−2308.
25. Vermillion, J. L., Balloou, D. P., Massey, V., and Coon, M. J. (1981) *J. Biol. Chem. 256*, 266−277.
26. Gachhui, R., Presta, A., Bentley, D. F., Abu-Soud, H. M., McArthur, R., Brudvig, G., Ghosh, D. K., and Stuehr, D. J. (1996) *J. Biol. Chem. 271*, 20594−20602.
27. Iyanagi, T., Makino, N., and Mason, H. S. (1974) *Biochemistry 13*, 1701−1710.
28. Noble, M. A., Munro, A. W., Rivers, S. L., Robledo, L., Daff, S., Yellowlees, L. J., Shimizu, T., Sagami, I., Gullemette, G., and Chapman, S. K. (1999) *J. Biol. Chem. 38*, 16413−16418.
29. Adak, S., Ghosh, S., Abu-Soud, H. M., and Stuehr, D. J. (1999) *J. Biol. Chem. 274*, 22313−22320.
30. Daff, S., Sagami, I., and Shimizu, T. (1999) *J. Biol. Chem. 274*, 30589−30595.
31. Klatt, P., Heinzel, B., John, M., Kastner, M., Bohme, E., and Mayer, B. (1992) *J. Biol. Chem. 267*, 11374−11378.
32. Williams, C. H. J., and Kamin, H. (1962) *J. Biol. Chem. 237*, 587−595.
33. Wolff, D. J., Datto, G. A., Samatovicz, R. A., and Tempsick, R. A. (1993) *J. Biol. Chem. 268*, 9425−9429.
34. Roman, L. J., Martasek, P., Miller, T., Harris, D. E., de la Garza, M. A., Shea, T. M., Kim, J., and Siler Masters, B. S. (2000) *J. Biol. Chem. 275*, 29225−29232.
35. Salerno, J. C., Harris, D. E., Irizarry, K., Patel, B., Morales, A. J., Smith, S. M., Martasek, P., Roman, L. J., Masters, B. S., Jones, C. L., Weissman, B. A., Lane, P., Liu, Q., and Gross, S. S. (1997) *J. Biol. Chem. 272*, 29769−29777.
36. Chen, P., and Wu, K. K. (2000) *J. Biol. Chem. 275*, 13155−13163.
37. Roman, L., Miller, T., de la Garaza, M., and Kim, J. (2000) *J. Biol. Chem. 275*, 21914−21919.
38. Nishida, C. R., and Ortiz de Montellano, P. R. (1998) *J. Biol. Chem. 273*, 5566−5571.

39. Dawson, V. L., and Dawson, T. M. (1996) *Neurochem. Int. 29*, 97−110.
40. Muchmore, D. C., McIntosh, L. P., Russell, C. B., Anderson, D. E., and Dahlquist, F. W. (1989) *Methods Enzymol. 177*, 44−73.
41. Gerber, N. C., and Ortiz de Montellano, P. R. (1995) *J. Biol. Chem. 270*, 17791−17796.
42. Stuehr, D. J., Cho, H. J., Kwon, N. S., Weise, M. F., and Nathan, C. F. (1991) *Proc. Natl. Acad. Sci. U.S.A. 88*, 7773−7777.
43. Peterson, G. (1977) *Anal. Biochem. 83*, 346−356.
44. Gelder, B. F. V., and Slater, E. C. (1962) *Biochim. Biophys. Acta 58*, 593−595.
45. Renosto, F., Ornitz, D. M., Peterson, D., and Segal, I. H. (1981) *J. Biol. Chem. 25*, 8616−8625.
46. Cleland, W. W. (1977) *Adv. Enzymol. Relat. Areas Mol. Biol. 45*, 273−387.
47. Cleland, W. W. (1963) *Biochim. Biophys. Acta 67*, 104−137.
48. Stuehr, D. J., Cho, H. J., Kwon, N. S., Weise, M. F., and Nathan, C. F. (1991) *Proc. Natl. Acad. Sci. U.S.A. 88*, 7773−7777.
49. Wolff, D. J., and Datto, G. A. (1992) *Biochem. J. 285*, 201−206.
50. Sem, D., and Kasper, C. (1994) *Biochemistry 33*, 12012−12021.
51. Northrop, D. B. (1969) *J. Biol. Chem. 244*, 5808−5819.
52. Cleland, W. W. (1963) *Biochim. Biophys. Acta 67*, 188−196.
53. Abu-Soud, H. M., Feldman, P. L., Clark, P., and Stuehr, D. J. (1994) *J. Biol. Chem. 269*, 32318−32326.
54. Miller, T. R., Martasek, P., Omura, T., and Siler Masters, B. S. (1999) *Biochem. Biophys. Res. Commun. 265*, 184−188.
55. Barden, R. E., Fung, C.-H., Utter, M. F., and Scrutton, M. C. (1981) *J. Biol. Chem. 247*, 1323−1333.
56. Tsai, C. S., Burgett, M. W., and Reed, L. J. (1973) *J. Biol. Chem. 248*, 8348−8352.
57. Coughlan, M. P., and Rajagopalan, K. V. (1980) *Eur. J. Biochem. 105*, 81−84.
58. Rendina, A. R., and Orme-Johnson, W. H. (1978) *Biochemistry 17*, 5388−5393.
59. Livingston, D. J., Fox, J. A., Orme-Johnson, W. H., and Walsh, C. T. (1987) *Biochemistry 26*, 4228−4237.
60. Arp, D. J., and Burris, R. H. (1981) *Biochemistry 20*, 2234−2240.
61. Hines, V., and Johnston, M. (1989) *Biochemistry 28*, 1222−1226.
62. Sem, D., and Kasper, C. (1995) *Biochemistry 34*, 12768−12774.
63. Murataliev, M. B., Klein, M., Fulco, A. J., and Feyereisen, R. (1997) *Biochemistry 36*, 8401−8412.
64. Labeth, J. D., and Klamin, H. (1976) *J. Biol. Chem. 251*, 4299−4306.
65. Wang, M., Roberts, D. L., Paschke, R., Shea, T. M., Masters, B. S., and Kim, J. J. (1997) *Proc. Natl. Acad. Sci. U.S.A. 94*, 8411−8416.
66. Karplus, P. A., Daniels, M. J., and Herriott, J. R. (1991) *Science 251*, 60−66.
67. Deng, Z., Alivert, A., Zanetti, G., Arakak, A. K., Ottado, J., Orellano, E. G., Clacaterra, N. B., Ceccarelli, E. A., Carrillo, N., and Karplus, P. A. (1999) *Nat. Struct. Biol. 6*, 847−853.
68. Cha, S. (1968) *J. Biol. Chem. 243*, 820−825.

BI0023495